# Alginate and cucurbit[*n*]uril as combined drug delivery system for albendazole: Experiments and mathematical modelling

**Wei Lu**

**A thesis submitted in fulfilment of the requirements for the degree of**

**Master of Philosophy**


**School of Physical, Environmental and Mathematical Sciences**

**University of New South Wales, Canberra**

**August, 2013**

**ORIGINALITY STATEMENT**

'I hereby declare that this submission is my own work and to the best of my knowledge it contains no materials previously published or written by another person, or substantial proportions of material which have been accepted for the award of any other degree or diploma at UNSW or any other educational institution, except where due acknowledgement is made in the thesis. Any contribution made to the research by others, with whom I have worked at UNSW or elsewhere, is explicitly acknowledged in the thesis. I also declare that the intellectual content of this thesis is the product of my own work, except to the extent that assistance from others in the project's design and conception or in style, presentation and linguistic expression is acknowledged.'

Signed Wei Lu .....

Date 22/11/2013 .....

**COPYRIGHT STATEMENT**

'I hereby grant the University of New South Wales or its agents the right to archive and to make available my thesis or dissertation in whole or part in the University libraries in all forms of media, now or here after known, subject to the provisions of the Copyright Act 1968. I retain all proprietary rights, such as patent rights. I also retain the right to use in future works (such as articles or books) all or part of this thesis or dissertation.
I also authorise University Microfilms to use the 350 word abstract of my thesis in Dissertation Abstract International (this is applicable to doctoral theses only).
I have either used no substantial portions of copyright material in my thesis or I have obtained permission to use copyright material; where permission has not been granted I have applied/will apply for a partial restriction of the digital copy of my thesis or dissertation.'

Signed Wei Lu .....

Date 22/11/2013 .....

**AUTHENTICITY STATEMENT**

'I certify that the Library deposit digital copy is a direct equivalent of the final officially approved version of my thesis. No emendation of content has occurred and if there are any minor variations in formatting, they are the result of the conversion to digital format.'

Signed Wei Lu .....

Date 22/11/2013 .....

# Contents

## List of Tables

# List of Figures

# ACKNOWLEDGEMENT

I would like to express my deepest appreciation to all those who provided me the possibility to complete this thesis.

I am the most grateful to my supervisors Dr. Anthony Day and A/Prof. Cliff Woodward for their guidance and support through my study at UNSW Canberra. My supervisor Anthony led me into the field of Supramolecular Chemistry and had great patience in our discussions on the experimental difficulties. In addition, his sense of humor has always inspired me in overcoming the frustrations. My joint-supervisor Cliff provided excellent guidance in the theoretical part of the project. I am amazed at his agility in extracting the most meaningful information out of complicated equations. I am also thankful to their proof reading and polishing my draft of this thesis.

Dr. Barry Gray provided me induction and continuous assistance on NMR studies. I would also like to thank all the staff at the School of PEMS for their help.

I received kind advices on laboratory skills and methods from the PhD students. I would like to express my gratitude to those helped me in dealing with the practical problems.

Last but not the least, my deepest appreciation is extended to my parents and friends for their support throughout my studies.

# ABSTRACT

A combined hydrogel-based drug delivery system consisting of alginate and cucurbit[*n*]uril (Q[*n*]) was prepared for the delivery of albendazole (ABZ), a sparingly soluble anthelmintic recently found to have anti-cancer activity. Q[*n*] is a family of macrocyclic host molecules that has two roles in the delivery system described within this thesis. The smaller homologue, Q[5], served as an ionic cross-linker with two sodium ions bonded at both of its portals. The larger homologues, Q[7] and Q[8], encapsulated ABZ in their cavities. The encapsulation significantly increased the solubility of ABZ in water and achieved considerable drug loading content within the hydrogel, with a relatively high loading efficiency around 40%.

Precursor solutions were prepared by dissolving sodium alginate in saturated Q[5] solutions. Different amounts of the drug complexes were dissolved to give precursor solutions of different formulation. The hydrogel beads were best form by dripping the precursor solutions into a pH1 gelling solution. The beads exhibited the same pH responsive swelling behaviour as calcium alginate hydrogel.

Drug release studies were conducted in release media of low and high NaCl concentrations at three pH conditions of 6.3, 3 and 1. Percentage of the loaded drug released and drug release rates were found to be highly sensitive to the concentration of NaCl and pH but were also affected by other factors such as the type (size of the homologue used) and the amount of the drug complexes loaded into the gel. Complete release of the drug could be achieved only in the presence of ions, suggesting substantial electrostatic attraction between the drug complexes, the cross-linking Q[5] and the alginate.

Experimental drug release data were analysed by mathematical models, which suggested that drug release was primarily controlled by diffusion, with a swelling controlled component, where ions were present. The fitted effective diffusion coefficient of the drug complexes ranged between ~$3\times10^{-8}$ and $7\times10^{-7}$ $cm^2/s$, depending on the type and the amount of the drug complexes loaded and the nature of the release media.

It is proposed, based on the experimental results and the mathematical modelling, that both of the drug complexes formed aggregates with Q[5] through intermolecular interactions, which is a process initiated by electrostatic attraction. However, ABZ@Q[8] had stronger interactions and formed larger aggregates than ABZ@Q[7], and hence had a more retarded release.

Slow release of ABZ over a few days was achieved in physiological saline with ABZ@Q[8] and ABZ@Q[7] offered faster release maintaining higher concentrations.

# Chapter 1 Introduction

## 1.1 Hydrogels and their applications

### 1.1.1 Definition

The terms hydrogel and hydrosol were introduced for the gelatinous and liquid hydrates of silicic acid, respectively, by Thomas Graham when reporting his studies on properties of silicic acid and its unusual diffusion behaviour [1, 2]. Materials that have vastly different structures are studied and referred to as 'gel' in different disciplines ever since, and a consensus of the definition is not reached [3]. K. Almdal et al. proposed a phenomenological definition of the term 'gel' [3] based on Ferry's definition [4], with the inclusion of certain viscoelastic liquids proposed by Burchard and Ross-Murphy[5]:

(1) A gel is a soft, solid or solid-like material of two or more components one of which is a liquid, present in substantial quantity.
(2) Solid-like gels are characterized by the absence of an equilibrium modulus, by a storage modulus, G'(ω), which exhibits a pronounced plateau extending to times at least of the order of seconds, and by a loss modulus, G''(ω), which is considerably smaller than the storage modulus in the plateau region.

According to K. Almdal et al., the solid-like characteristic of gels should be directly observable to humans, i.e. the material should be elastic and resilient to human touch and should not flow under its own weight at least on a time scale of seconds [3]. All the hydrogels discussed in this work satisfy the criteria stated above.

From a structural point of view, it is widely accepted that hydrogels are hydrophilic three-dimensional networks formed by cross-linking water soluble polymers [6-10]. Due to hydrophilic groups or domains present in the polymeric network, hydrogels are capable of imbibing water or biological fluids up to thousands of times their dry weight. Meanwhile, hydrogels remain insoluble because chemical or physical cross-links are present, providing network structure and physical integrity [7].

### 1.1.2 Classification

Due to the wide range of water soluble polymers and diverse cross-linking methods, hydrogels are a large family of materials having a myriad of chemical compositions and hence different

physical properties. As a result, there are a number of ways to classify hydrogels, among which classifications by polymer origin or cross-linking method provide the most meaningful insight into hydrogel properties.

Hydrogels can be classified as natural or synthetic based on the origin of the water soluble polymer. Generally, hydrogels made from natural polymers possess inherent biocompatibility, degradability and potentially biologically recognizable moieties to promote cell adhesion or enhanced enzymatic activity [9, 11]. Despite these advantages, natural hydrogels suffer from several drawbacks such as low mechanical strength, potential for evoking immune/inflammatory responses and pathogen contamination [9]. Batch differences in properties and key parameters of naturally derived hydrogels also make comparisons between different studies difficult [11].

Synthetic hydrogels, on the other hand, offer better mechanical properties and extensive versatility that can be tailored to meet specific needs. Given the abundance of monomers and cross-linking methods, synthetic hydrogels can be designed to play niche roles in different applications. For example, chemical cross-links labile to enzymatic or hydrolytic degradation can be introduced to achieve a controllable degradation rate [12, 13]. Many synthetic hydrogels, e.g. poly(ethylene glycol) (PEG) and poly(vinyl alcohol) (PVA), are biocompatible and biological cues such as the Arginine-Glycine-Aspartic acid (RGD) tri-peptide can be incorporated to promote cell adhesion[8, 9]. However, residual initiators, cross-linkers, unreacted monomers and oligomers in synthetic hydrogels may be toxic and have to be extracted before application [7]. Moreover, harsh conditions for synthetic hydrogel preparation are likely to damage fragile biomacromolecules such as proteins, DNA and peptides once they are present [6, 7]. Table 1.1 lists natural and synthetic monomers that are most often used in hydrogel fabrication [7, 9].

**Table 1.1 Natural polymers and synthetic monomers most often used in hydrogel fabrication [7, 9].**

| Natural polymer | Synthetic monomer | Monomer abbreviation |
|---|---|---|
| Alginate | Hydroxyethyl methacrylate | HEMA |
| Carrageenan | Hydroxyethoxyethyl methacrylate | HEEMA |
| Chitosan | Hydroxydiethoxyethyl methacrylate | HDEEMA |
| Collagen | Methoxyethyl methacrylate | MEMA |
| Dextran | Methoxyethoxyethyl methacrylate | MEEMA |
| Fibrin | Methoxydiethoxyethyl methacrylate | MDEEMA |
| Gelatin | Ethylene glycol dimethacrylate | EGDMA |
| Hyaluronic acid | *N*-vinyl-2-pyrrolidone | NVP |
| | *N*-isopropyl acrylamide | NIPAAm |
| | Vinyl acetate | VAc |
| | Acrylic acid | AA |
| | Methyl methacrylate | MAA |
| | *N*-(2-hydroxypropyl) methacrylamide | HPMA |
| | Ethylene glycol | EG |
| | PEG acrylate | PEGA |
| | PEG methacrylate | PEGMA |
| | PEG diacrylate | PEGDA |
| | PEG dimethacrylate | PEGDMA |

Hydrogels can also be classified by the cross-linking method. Physical cross-linking includes ionic interactions, crystallization, stereocomplex formation, hydrophobic interactions, hydrogen bonds, protein interactions, supramolecular chemistry and molecular entanglements [6, 8, 10]. Some excellent examples of physical cross-linking are alginate gel cross-linked by $Ca^{2+}$ [14-16], PVA gel prepared by freeze-thaw cycles [17, 18], stereocomplex formation of PLLA and PDLA (the homopolymers of L-lactic acid and D-lactic acid, respectively) [19], and reverse thermal gelation of tri-block copolymers of poly(ethylene oxide)-poly(propylene oxide)-poly(ethylene oxide) (PEO-PPO-PEO, the Pluronic or Poloxamer series) through the

hydrophobic interaction of PPO blocks when the temperature is between two critical transition values, the lower being a sol to gel transition and the higher being a gel to sol transition [20].

Generally, physical cross-links are reversible and hydrogel networks held by them disintegrate rather quickly in the surrounding media. When linear polymers are cross-linked through covalent bonds by cross-linkers, chemically cross-linked hydrogels are formed. Although chemically cross-linked hydrogels offer better mechanical properties and robustness in most cases, it is often desirable that they are degradable for biomedical applications [6]. This can be achieved by either employing reversible cross-links or introducing degradability to the polymer backbone or both. For example, reversible ester and amide bonds are widely applied as cross-linking bonds [10, 13, 21, 22] and alginate is made degradable in aqueous media by slight oxidation [23]. A number of chemistries have been explored for the fabrication of chemically cross-linked hydrogels. Chemical reaction of functional groups present in both the linear polymer (mainly hydroxyl, carboxyl or amine groups) and the cross-linker is utilized to form hydrogels. For example, PVA can be cross-linked by glutaraldehyde under rather drastic conditions [6, 24]. Polymers containing amine groups (e.g. chitosan), however, can be cross-linked by dialdehydes forming the so-called Schiff base under mild conditions [6, 25]. The major drawback of the dialdehyde cross-linkers is toxicity. Glutaraldehyde inhibits cell-growth even at low concentrations and glyoxal is mutagenic [6, 25]. Genipin, a naturally occurring cross-linker, or polyaldehydes are promising substitutes for dialdehydes [6, 11]. In the presence of appropriate cross-linking agents (e.g. glycol dimethacrylate), radical polymerization of hydroxyethyl methacrylate (HEMA) results in an inert hydrogel difficult to hydrolyse [26]. Stimuli sensitive hydrogels were synthesized by radical polymerization of *N*-isopropylacrylamide (NIPAAm) or acrylic acid (AAc) or their mixture with the presence of bis (or higher) functional cross-linking agents such as *N*, *N*'-methylenebis(acrylamide)[6, 11]. Macroradicals and hydroxyl radicals can be formed through the homolytic scission of polymers and radiolysis of water molecules, respectively, when high energy irradiation is applied to polymer solutions [6]. A cross-linked network emerges as the macroradicals recombine [6]. In this way, radiation dose is introduced as a unique and easily controllable parameter to manipulate the properties of hydrogels. Sperinde et al. reported the formation of a hydrogel through enzymatic cross-linking where poly(ethylene glycol) (PEG) functionalized with glutaminamide was cross-linked by a lysine-containing polypeptide [27]. This approach offers well controlled gelation kinetics and is suitable for *in situ* gelling. The activity of the enzyme used, transglutaminase, is $Ca^{2+}$ dependent. Westhaus et al. used liposomes to effectively entrap $Ca^{2+}$ under ambient temperature. $Ca^{2+}$ was released rapidly when liposomes were

heated to body temperature. Transglutaminase in the precursor solution was then activated to covalently cross-link fibrinogen [28].

Hydrogels can also be classified to be neutral, anionic or cationic according to their side groups. Based on their mechanical and structural characteristics, they can be affine or phantom networks [7]. For an affine network, the cross-links displace linearly with the macroscopic deformation and do not fluctuate; for a phantom network, the cross-links fluctuate over time [29]. Hydrogels can be macro-porous, micro-porous or non-porous based on the space available between polymer chains, which is regarded as the 'pore'. They can be homopolymer or copolymer networks based on the kinds of monomers used [7].

### 1.1.3 Network structure and key parameters

The most significant difference of hydrogels from hydrophobic polymeric networks is their hydrophilicity and this is where their myriad applications stem from. Characterization of the amount of water hydrogels can retain, or even further their network structures, is essential for choosing or designing a hydrogel for a particular application. Three critical parameters, polymer volume fraction in the swollen state ($v_{2,s}$), number average molecular weight between two neighbouring cross-links ($\bar{M}_c$), and network mesh size ($\xi$), are generally used to describe the network structure of hydrogels [7, 9].

#### 1.1.3.1 Polymer volume fraction in the swollen state

The polymer volume fraction in the swollen state is a ratio of the polymer volume ($V_p$) to the swollen gel volume ($V_g$), and is a measure of the amount of liquid imbibed in hydrogels [7, 9]. It is the reciprocal of volumetric swollen ratio ($Q$) which can be calculated from the experimentally measurable mass swollen ratio ($Q_m$), when the densities of the swelling medium ($\rho_1$) and polymer ($\rho_2$) are known. The mass swollen ratio ($Q_m$) is defined as the mass ratio of imbibed liquid and the polymer. The relationships of these parameters are described by equation (1.1):

$$v_{2,s} = \frac{V_p}{V_g} = Q^{-1} = \frac{1/\rho_2}{Q_m/\rho_1 + 1/\rho_2} \qquad (1.1)$$

#### 1.1.3.2 Average molecular weight between two consecutive cross-links

The degree of cross-linking of the hydrogel network is measured by the average molecular weight between two adjacent cross-links ($\bar{M}_c$). The equilibrium swelling theory and the

rubber elasticity theory are two prominent methods used to elucidate the relationship between $\overline{M}_c$ and other measured parameters [7].

If a hydrogel does not contain ionic moieties, its equilibrium with surrounding liquid can be described by the thermodynamic Flory-Rehner theory. This theory suggests that the hydrogel immersed in a fluid is only subject to two opposing forces, the thermodynamic force of mixing and the retractive force of polymer chains [7]. At equilibrium, the two forces balance each other, and the chemical potentials of the solvent outside and inside the gel are equal. Changes of chemical potential induced by mixing and elastic retractive forces can be expressed using heat and entropy of mixing and the rubber elasticity theory, respectively. Equation (1.2) can be derived to calculate the average molecular weight between two consecutive cross-links ( $\overline{M}_c$ ) of a neutral hydrogel prepared without a solvent, upon equating these two contributions [7, 9].

$$\frac{1}{\overline{M}_c} = \frac{2}{\overline{M}_n} - \frac{(\overline{v}/V_1)\left[\ln\left(1-v_{2,s}\right)+v_{2,s}+\chi_1 v_{2,s}^2\right]}{v_{2,s}^{1/3}-v_{2,s}/2} \quad (1.2)$$

The original Flory-Rehner equation is modified for hydrogels prepared in the presence of a solvent by Peppas and Merrill [30]. Change of chemical potential due to elastic forces now involves the volume fraction density of polymer chains during cross-linking. Equation (1.3) is the modified equation for predicting the average molecular weight between two adjacent cross-links ( $\overline{M}_c$ ) of a neutral hydrogel prepared in a solvent.

$$\frac{1}{\overline{M}_c} = \frac{2}{\overline{M}_n} - \frac{(\overline{v}/V_1)\left[\ln\left(1-v_{2,s}\right)+v_{2,s}+\chi_1 v_{2,s}^2\right]}{v_{2,r}\left[\left(\frac{v_{2,s}}{v_{2,r}}\right)^{1/3}-\left(\frac{v_{2,s}}{2v_{2,r}}\right)\right]} \quad (1.3)$$

In the two equations above, $\overline{M}_n$ is the number average molecular weight of the linear polymer chain without cross-linking, $\overline{v}$ is the specific volume of the polymer, $V_1$ is the molar volume of the swelling agent, $\chi_1$ is the Flory polymer-swelling agent interaction parameter of the particular polymer, and $v_{2,r}$ is the polymer fraction in the relaxed state, which is the state of the hydrogel immediately after cross-linking but before swelling.

If ionic moieties are present in a hydrogel, the change of chemical potential must include the additional contribution of the ionic character of the network, which makes the theoretical treatment much more complex. Peppas et al. developed expressions for the swelling of anionic

and cationic hydrogels prepared with solvent present [31], as shown in equation (1.4) and (1.5), respectively.

$$\frac{V_1}{4I}\left(\frac{\upsilon_{2,s}}{\bar{\upsilon}}\right)^2\left(\frac{K_a}{10^{-\mathrm{pH}}+K_a}\right)^2 = \ln(1-\upsilon_{2,s})+\upsilon_{2,s}+\chi_1\upsilon_{2,s}^2+\left(\frac{V_1}{\bar{\upsilon}\bar{M}_c}\right)\left(1-\frac{2\bar{M}_c}{\bar{M}_n}\right)\upsilon_{2,r}\left[\left(\frac{\upsilon_{2,s}}{\upsilon_{2,r}}\right)^{1/3}-\left(\frac{\upsilon_{2,s}}{2\upsilon_{2,r}}\right)\right] \quad (1.4)$$

$$\frac{V_1}{4I}\left(\frac{\upsilon_{2,s}}{\bar{\upsilon}}\right)^2\left(\frac{K_b}{10^{\mathrm{pH}-14}+K_b}\right)^2 = \ln(1-\upsilon_{2,s})+\upsilon_{2,s}+\chi_1\upsilon_{2,s}^2+\left(\frac{V_1}{\bar{\upsilon}\bar{M}_c}\right)\left(1-\frac{2\bar{M}_c}{\bar{M}_n}\right)\upsilon_{2,r}\left[\left(\frac{\upsilon_{2,s}}{\upsilon_{2,r}}\right)^{1/3}-\left(\frac{\upsilon_{2,s}}{2\upsilon_{2,r}}\right)\right] \quad (1.5)$$

Here, $I$ is the ionic strength of the swelling medium, and $K_a$ and $K_b$ are the dissociation constants for the anionic and cationic polyelectrolyte, respectively. As indicated by these equations, the swelling of ionic hydrogels depends strongly on the ionic strength and on the nature of the ions present.

Most hydrogels in their swollen state exhibit rubber elastic behaviour which is characterized by high extensibility generated by low mechanical stress, fully reversible deformation, and entropy rather than enthalpy driven elasticity [7, 32]. Relationships between network structure and mechanical stress-strain behaviour can be derived using statistical thermodynamics, which is given by equation (1.6) [32].

$$\tau = \frac{\rho RT}{\bar{M}_c}\frac{\bar{r}_o^2}{\bar{r}_f^2}\left(1-\frac{2\bar{M}_c}{\bar{M}_n}\right)\left(\lambda-\frac{1}{\lambda^2}\right) \quad (1.6)$$

Here, $\tau$ is the stress applied to the hydrogel sample, $\rho$ is the density of the polymer which should be interpreted as a concentration in hydrogels, $R$ is the universal gas constant and $T$ is the absolute temperature. $\bar{r}_o^2$ and $\bar{r}_f^2$ are the root-mean-square, unperturbed, end-to-end distance of the polymer chains between two consecutive cross-links and of isolated chains, respectively, and their ratio is referred to as the front factor. $\lambda$ is the elongation ratio which is the ratio of the dimension after and before deformation.

In the case where the front factor is unknown, it is often approximated as 1 [32]. The term $\left(1-\frac{2\bar{M}_c}{\bar{M}_n}\right)$ is introduced to correct network imperfections such as cycles and chain entanglements, and is negligible when $\bar{M}_n \gg \bar{M}_c$ [32]. Under such circumstances, let

$$G = \frac{\rho RT}{\bar{M}_c} \tag{1.7}$$

We have

$$\tau = G\left(\lambda - \frac{1}{\lambda^2}\right) \tag{1.8}$$

If the hydrogel is isotropic and deformation is small $(\lambda \approx 1)$, a close examination of equation (1.8) will give $E = 3G$, which is the relationship between the tensile modulus and shear modulus for an isotropic rubber whose Poisson's ratio is about 0.5. Therefore, $G$ is effectively the shear modulus of an isotropic hydrogel when the strain is small. The value of the shear modulus can be obtained from tensile tests [7], compressive tests [21, 32, 33], or dynamic mechanical analysis, as demonstrated by Meyvis et al. [34]. The average molecular weight between two consecutive cross-links ($\bar{M}_c$) can be calculated using equation (1.7) with the knowledge of the shear modulus ($G$).

Another convenient method to calculate the average molecular weight between adjacent cross-links ($\bar{M}_c$) for neutral hydrogels at highly swollen conditions $(Q > 10)$ is from the volumetric swollen ratio ($Q$), as shown by equation (1.9) [9]. This is derived from a simplified form of the Flory-Rehner equation.

$$Q^{\frac{5}{3}} = \upsilon_{2,s}^{-\frac{5}{3}} = \frac{\bar{\upsilon}\bar{M}_c\left(1/2 - \chi_1\right)}{V_1} \tag{1.9}$$

### 1.1.3.3 Network mesh size

The last important parameter is the network mesh size ($\xi$), which is the correlation distance between cross-links and describes the size of the pores of the hydrogel, indicating the upper limit of solutes that can pass through it [35]. It can be calculated using equations (1.10) and (1.11), with the knowledge of $\bar{M}_c$ and $v_{2,s}$.

$$\xi = \lambda\left(\overline{r}_o^2\right)^{1/2} = \upsilon_{2,s}^{-1/3}\left(\overline{r}_o^2\right)^{1/2} = Q^{1/3}\left(\overline{r}_o^2\right)^{1/2} \qquad (1.10)$$

$$\left(\overline{r}_o^2\right)^{1/2} = l(C_n N)^{1/2} = l\left(C_n \frac{2\overline{M}_c}{M_r}\right)^{1/2} \qquad (1.11)$$

Here, $l$ is the bond length along the polymer backbone, $C_n$ is the Flory characteristic ratio, $N$ is the number of bonds between cross-links, and $M_r$ is the molecular weight of the polymer's repeating unit.

It is seen in equations (1.9) and (1.11) that both $Q$ and $\overline{r}_o^2$ are proportional to $\overline{M}_c$ raised to a certain power. Therefore, combining equations (1.9)-(1.11), we have

$$\xi = Q^{1/3}\left(\overline{r}_o^2\right)^{1/2} \sim \left(\overline{M}_c\right)^{7/10} \qquad (1.12)$$

and this is called the scaling law [35, 36].

Schurz et al. developed an "equivalent network model" to estimate the network mesh size from $\overline{M}_c$, where a collection of "blobs" of diameter $\xi$ represents the entangled network structure [37]. Equation(1.13) gives the calculation of $\xi$ with this model.

$$\xi = \sqrt[3]{\frac{6\overline{M}_c}{\pi c N_A}} \qquad (1.13)$$

Here, $c$ is the polymer concentration and $N_A$ is Avogadro's number.

### 1.1.4 Applications of hydrogels

There has been a growing interest in hydrogels since Wichterle and Lim [26] published their pioneering work on cross-linked HEMA hydrogels in 1960, where compatibility with living tissue was emphasized. The advance in hydrogels promoted their applications in different fields such as tissue engineering, drug delivery, biomedical implants, biosensors and BioMEMS devices. W. Lee et al. reported surface modification of a protein-repellent PEG hydrogel via graft polymerization of acrylic acid induced by photolithography. Carboxyl groups of the well-defined, pH-responsive poly(acrylic acid) (PAA) were activated by immersion into a solution of EDC (1-ethyl-3-(3-dimethylaminopropyl)carbodiimide) and NHS (*N*-hydroxysuccinimide). Albumin was covalently attached to the micropattern through amide formation while the unpatterned hydrogel surface effectively prevented non-specific adsorption [38].

Micropatterns were created on oxidized silicon wafer by cross-linking the thermo-sensitive PNIPAAm-based copolymer photolithographically. Transition time was determined to be 2 to 8 seconds with the swelling ratio in the same magnitude of bulk PNIPAAm-based gels, proving the hydrogel suitable as a working material in microactuators [39]. Hydrogels that reversibly swell-contract in response to external stimuli may also serve as flow control devices in microfluidics [40, 41].

#### 1.1.4.1 Application in tissue engineering

Tissue engineering is an interdisciplinary field that aims at developing biological substitutes to restore, maintain, or improve functions of diseased tissue or organ [42], instead of transplanting harvested tissues and organs. The strategy adopted is to place cells on or within three-dimensional matrices which allow cell attachment, proliferation and differentiation. Hydrogels are especially attractive to tissue engineering as cell-encapsulating matrices, due to their high biocompatibility resulting from their high water content and their compositional and mechanical similarity to the extracellular matrix (ECM) [8]. However, Kohane and Langer emphasized on evaluating the biocompatibility of a material for individual applications, rather than regarding it as intrinsic to the material [43]. Another desirable property of the matrices, or “scaffolds”, is that their architectural or other functions are time-limited and will be handed over to the newly formed tissue or organ through their gradual degradation. Other properties may also be critical to the success of a material for a particular target site and delivered cells, including mechanical properties, cell adhesion properties, and the ability to induce cell differentiation.

Many approaches utilizing a wide range of technologies have been applied to tune the properties of hydrogels to make them better suit specific applications. Mooney and co-workers used sodium periodate to prepare partially oxidized alginate. It was capable of forming a hydrogel by cross-linking with calcium ions as do ordinary alginate. This 5% oxidized alginate gel hydrolysed to yield low molecular weight oligomers in aqueous solutions with a rate dependent on pH and temperature, while ordinary alginate is non-degradable and thus is difficult to be cleared from the body. Moreover, cartilage-like tissue formation was found improved greatly in vivo with partially oxidized alginate gel, as its degradation left enough space for in-growth of extracellular matrix [23].

Kuo and Ma demonstrated the effect of gelation rate on the homogeneity, syneresis behaviour, and mechanical integrity of calcium-alginate hydrogel. Gelation rate can be controlled by varying the molar ratio of calcium carbonate and calcium sulphate dihydrate, calcium content,

polymer concentration, and gelation temperature. Cell distribution was homogeneous and ensures uniform new tissue formation [44].

Hydrogel surfaces can be modified by naturally derived biomolecules to selectively induce cell adhesion, migration, and proliferation. Growth factors may be incorporated to promote angiogenesis and/or bone and cartilage regeneration [45].

#### 1.1.4.2 Application in drug delivery

Another extensive utilization of hydrogels lies in the broader field of controlled drug delivery. Cell-based drug delivery, where a variety of stem cells, progenitor cells, lineage-committed cells, and genetically engineered cells are transplanted to secrete therapeutic proteins and cytokines, suffers from low therapeutic efficacy due to a variety of reasons with the most significant ones being immune rejection and a rapid decrease in cell viability [46]. One promising strategy to overcome these problems is encapsulating the cells in permeable membranes or matrices. Access of immune cells to the transplanted cells is blocked by the matrices while the influx of nutrients and oxygen and efflux of secreted therapeutic molecules and cellular wastes are maintained [46]. Moreover, the encapsulating materials provide a proper microenvironment and mechanical support to the transplanted cells, preserving cell viability and functionality.

The requirements of the materials for such membranes or matrices are similar to tissue engineering and hydrogels is a common option. Immune response is mediated by the adsorption of proteins onto the materials' surface, which induces the subsequent recruitment of immune cells [46]. Furthermore, toxins present in the matrices may stimulate the secretion of cytokines and immunoglobulin which are detrimental to the encapsulated cells. Therefore, biocompatibility in this regard is protein repellence and minimal presence of toxins, which can be achieved by using biologically inert hydrogels, surface modification or coating of the hydrogel with bio-inert materials, and thoroughly removing the toxins present [46].

Transport properties and mechanical properties are also important to the success of a cell-encapsulating matrix, as alluded above. Surface and bulk pore sizes are critical to the transport properties, as they determine the molecular weight cut-off of the hydrogel. Surface pore size can be controlled by careful selection of hydrogel material and appropriate coating such as polyelectrolyte complex formation. Bulk pore size can be tuned through varying cross-linking density and modification of the chemical structure of the polymer used [46]. For example, PEG hydrogels prepared with poly(ethylene glycol) diacrylate (PEGDA) of molecular weights 2000,

4000 and 8000 were impermeable to proteins such as immunoglobulin, albumin and myoglobin (22kDa), but not vitamin B12 (1.3kDa). By increasing the molecular weight of PEGDA to 20000, diffusion of smaller proteins was enabled, but proteins with a size equal to or larger than ovalbumin (45kDa) remained impermeable [47]. This observation is in accordance with the calculated molecular weights between cross-links and mesh sizes, which were similar for hydrogels formed by PEG with molecular weight smaller than 8000 and were larger for that formed by PEG 20000 [47].

Mechanical properties of hydrogels involve stiffness, toughness, and structural integrity over time. Stiffness describes the ability of a material to resist deformation. This can be enhanced by increasing polymer concentration and cross-linking density. However, for covalently cross-linked hydrogels, the increase in stiffness is generally accompanied by the decrease in toughness [46], which is undesirable as hydrogels become susceptible to failure especially under abrupt or cyclic mechanical stresses. It is thus important that these two properties are decoupled. Ionic cross-links may be a solution as both stiffness and toughness were increased with the increasing cross-linking density in calcium-alginate hydrogels [48]. It is also worth noting that mechanical properties of the hydrogel can serve as biological cues and have influence on function, differentiation pathway, and even the fate of the encapsulated cells [49]. The long-term stability is particularly important for ionically cross-linked hydrogels, because ion-exchange with other ions present in the environment leads to a gradual decrease of the stiffness of such hydrogels [21, 48]. The strategy of coating these hydrogels by polyelectrolyte complex formation was applied to enhance durability [46, 50]. The long-term structural integrity may be further improved with interpenetrating networks or semi-interpenetrating networks [46, 50].

The cell encapsulation process affects cell viability greatly and can be categorized as macroencapsulation and microencapsulation, depending on the amount of cells encapsulated in a single piece of device [46]. Mixing cells with highly viscous solutions can physically damage cell membranes because of the high shear stress applied, and consequently decrease cell viability [46].

More generally, drugs can be encapsulated in polymeric matrices serving as drug delivery systems, which are engineered to release the loaded drug in a predefined manner [50]. In most cases, it is desirable that drug release is prolonged so that dosing frequencies are reduced. Ideally, the administration of loaded drug would be modulated temporally and/or be target specific [51]. “Drug” in this context means effectively any molecule with therapeutic

significance, ranging from small molecules to proteins and nucleic acids. Most macro biomolecules are susceptible to enzymatic degradation and experience short plasma circulation times and rapid renal clearance, leading to repeated administration in order to maintain an effective drug concentration [9]. Therefore, encapsulation of such biomolecules in polymeric matrices was proposed to protect these fragile molecules, improve their efficacy after administration, and avoid the side effects of repeated dosing. Hydrophilic matrices are superior to their hydrophobic counterparts in this respect as their relatively mild fabrication and drug encapsulation conditions better preserve the 3-D structure of the biomolecules. More recently, there is growing interest in controlled delivery of smaller drugs using hydrogels. One advantage of doing so is achieving high local concentrations without provoking systemic toxicity.

There are three major approaches to incorporate drugs into hydrogels [50]. The permeation method is to immerse fully formed hydrogel into a saturated therapeutic solution. Diffusion is the major driving force for drug absorption and the rate depends on the porosity of the hydrogel, the size of the drug, and the interaction between the two components. Although permeation is a relatively easy way of drug incorporation, it is ineffective in loading large therapeutics and is limited by its long drug loading time.

Alternatively, a drug can be mixed with the polymer precursor solution, allowing the simultaneous accomplishment of network formation and drug encapsulation in one process. The main risks of this drug loading scheme are the deactivation of the therapeutic agent during the cross-linking process and the presence of residual reactants.

To eliminate the burst release associated with the above methods and enable prolonged release, drugs can be tethered to the polymer chains via labile covalent bonds or drug-ligand interaction. Drug-polymer conjugates are created, followed by gelation of the precursor solution. These drug loading schemes and their comparison are summarized in Figure 1.1.

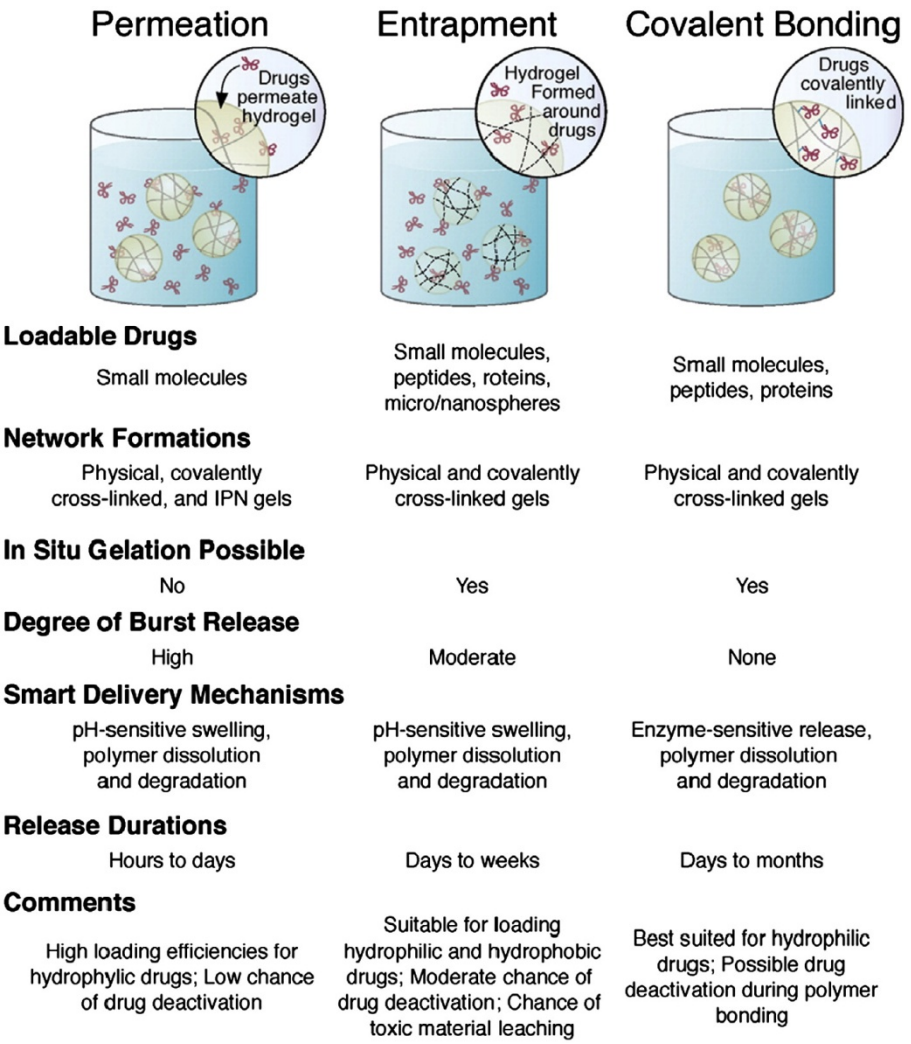


**Figure 1.1 Three different drug incorporation schemes and their comparison. Reproduced from [50].**

The strategy of drug incorporation, together with the physicochemical properties of the hydrogel, determines the release mechanism(s), which are roughly classified as diffusion-controlled, swelling- controlled, and chemically-controlled [7, 9].

Drug release from most hydrogel delivery systems can be described by diffusion-controlled models, where Fick's law of diffusion is commonly applied. For a matrix system where drug is homogeneously dispersed throughout, Fick's second law of diffusion is applied, with the general form:

$$\frac{\partial C_A}{\partial t} = \frac{\partial}{\partial x}\left( D(C_A)\frac{\partial C_A}{\partial x} \right) \qquad (1.14)$$

where $D(C_A)$ is the concentration-dependent diffusion coefficient of the drug, or can be assumed to be a constant for simplicity. The diffusion coefficient of the drug within the matrix

is related to the porosity and the tortuosity of the matrix, and steric hindrance must be taken into account when pore sizes are comparable to the molecular size of the drug [9]. Diffusion coefficients can be determined empirically or can be predicted by theoretical models that relate it to fundamental matrix characteristics and properties of the drug molecule. Such theoretical models are categorized as free volume theory, hydrodynamic theory, or obstruction theory, or some combination of them [52-54], and have the general form [9]:

$$\frac{D_g}{D_o} = f(r_s, v_{2,s}, \xi) \qquad (1.15)$$

Here, $D_g$ is the drug diffusion coefficient in the swollen matrix and $D_o$ is the same term in pure solvent. $r_s$ is the radius of the drug molecule. Analytical solutions of equation (1.14) can be derived for planar, cylindrical, or spherical matrices with proper initial and boundary conditions once the diffusion coefficient is determined [55]. It should be noted that only numerical solutions of equation (1.14) are feasible for more complex matrix geometries or concentration-dependant diffusion coefficients.

There are two major subclasses of chemically-controlled drug delivery systems, erodible systems and pendant chain systems [7, 9]. In erodible systems, drug release is controlled by the degradation or dissolution of the hydrogel, because drug molecules are trapped in the network and are not free for diffusion until hydrogel erodes. If hydrogel erosion is limited to the surface, it usually exhibits desirable near zero-order release kinetics [7]. In pendant chain systems, drug molecules are tethered on polymer chains through hydrolytically or enzymatically labile bonds, and drug release is controlled by the degradation of cleavable bonds. Diffusion is not the controlling step in either system, because diffusion of the drug molecules after hydrogel erosion or bond cleavage is assumed to be much faster than the rate of respective chemical process.

Drug release from swelling-controlled systems is governed by the inward flux of solvent and the associated swelling of the hydrogel [7]. These systems are usually prepared by compressing homogeneous powders of dry hydrogel, drug, and other excipients into tablets. Upon contact with swelling media, hydrogels undergo a swelling-driven phase transition from the glassy state into the rubbery state. Consequently, rapid diffusion of the immobile drug entrapped in the glassy state hydrogel is enabled in the rubbery state [7, 9]. The depletion of loaded drug is associated with the inward movement of the glassy-rubbery phase interface.

Polymer chain relaxation time is much longer than drug diffusion time in swelling-controlled systems [7]. Otherwise, the drug release is diffusion-controlled.

To further tune the drug release profile, combinations of the three release mechanisms have been applied to design delivery systems [9]. Moreover, triggered release responsive to external stimuli such as temperature, pH and electric signal have been realized [51]. It is even more fascinating that the release of therapeutics is responsive to physiological needs. In one approach, an antigen and the corresponding antibody were immobilized onto polymer chains. Hydrogel formation was achieved by antigen-antibody binding. Free antigens competed with polymer-bound antigens for the binding with antibody, and cross-linking density was decreased. Consequently, hydrogel swelled and led to rapid release of loaded drug [56].

In conclusion, biocompatibility, transport properties, mechanical properties, drug loading method and stimuli responsiveness all have an impact on the performance and release profile of drug delivery systems. Precisely matching the properties of the hydrogel to the physiological environments of the application site is critical to its success.

## 1.2 Alginate as drug delivery systems

### 1.2.1 Alginate and its structure

Alginate is a collective term for a family of naturally occurring linear unbranched polysaccharides isolated from brown seaweeds and certain bacteria. They are (1−4)-linked binary copolymers of *β*-D-mannuronate (M) and *α*-L-guluronate (G). The M and G units are C-5 epimers and are present in different amounts in alginate isolated from various sources. Homogeneous blocks composed of either unit alone are interdispersed with blocks of alternating mannuronate and guluronate units on the alginate chain. Figure 1.2 shows the structures of such blocks formed by diequatorial (MM), diaxial (GG), and equatorial-axial (MG) glycosidic linkages [14, 57-60]. More than 200 alginates differ in M and G unit contents and the length of each block are commercially available. Most of them are in the sodium salt form due to its solubility in cold water [59, 60].

Although there is still debate on the biocompatibility of alginate, it is generally accepted to be a highly biocompatible material, and negative examples were attributed to impurities rather than alginate itself or its mannuronate and guluronate composition [60]. Due to its biocompatibility, low toxicity, relative low cost and mild gelling conditions, alginate has found numerous applications in the food industry, pharmaceutics, biomedical implants and even sewerage treatment [11, 57, 61, 62].

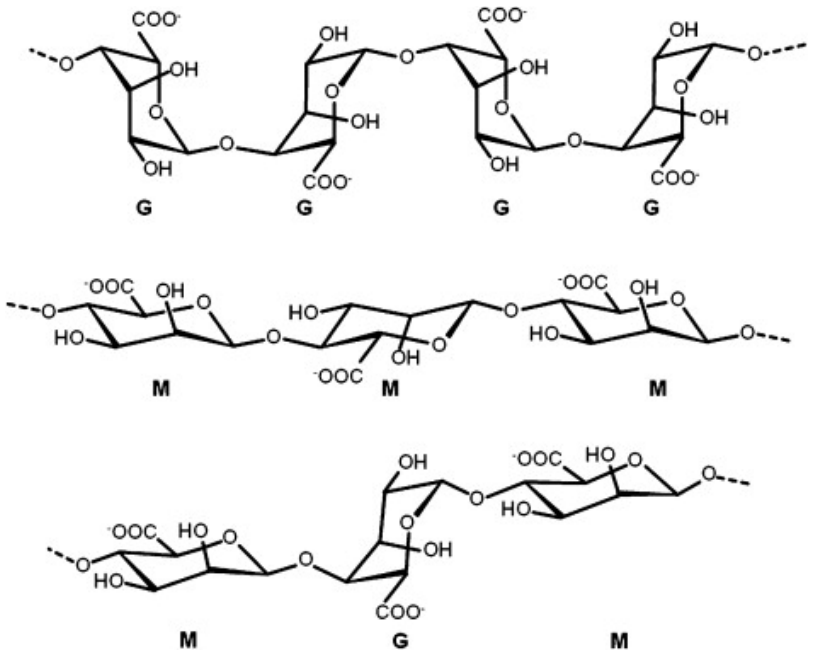


**Figure 1.2 Chemical structures of G-block, M-block and alternating block of alginate. Reproduced from [60].**

### 1.2.2 Common cross-linking methods and alginate hydrogel structures

A vast majority of the myriad alginate hydrogels prepared are cross-linked by divalent cations especially $Ca^{2+}$. This can be achieved by either dripping alginate solution into calcium salt solutions or dialysing with solutions containing the calcium cation. High concentrations of available $Ca^{2+}$, however, led to rapid and poorly controlled gelation and the resulting hydrogels are inhomogeneous and weak mechanically. There is a growing interest in fabricating homogeneous ionically cross-linked alginate hydrogels, through the utilization of inactive forms of calcium or moieties that compete with alginate for the binding of $Ca^{2+}$ [59, 60]. In one approach, a calcium carbonate suspension was mixed with glucono-δ-lactone (GDL) solution to serve as the cross-linking agent [44]. The slow hydrolysis of GDL decreased the pH and calcium ions were released gradually to initiate alginate gelation. The gelation rates can also be controlled by varying the particle size of the inactive calcium source and gelling temperature. Interestingly, alginate can form an acid gel by hydrogen bonds when the pH is low enough to enable the protonation of the carboxylate groups [14, 59], even in the absence of divalent cations.

The egg-box model proposed by Morris and co-workers [63] is the generally accepted description of the structure of calcium alginate hydrogel for more than 30 years [14]. Divalent cations bind solely to the G blocks in this model, where the G blocks assume a 2/1 zigzag helical conformation [63], as shown in Figure 1.3. This model was deduced from the structure of alginic acid gel, for which the clear X-ray diffraction pattern fully supports the two fold

helical structure of the G block [64]. The diffraction pattern for calcium alginate hydrogel, however, is very poor and not confirmative for the 2/1 egg-box model [14]. Therefore, this model has been questioned from different aspects by some researchers [14]. A recent study suggested that the 2/1 helix is metastable and only suitable for rapidly-gelled calcium alginate. A 3/1 helical conformation is more proper for slowly-gelled calcium alginate, as suggested by Li et al [14].

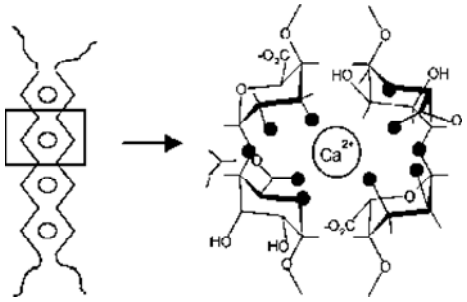


**Figure 1.3 Schematic illustration of the egg-box model for calcium alginate, as proposed by Morris et al. Reproduced from [14].**

Calcium alginate hydrogels have limited long-term structural integrity in physiological conditions due to ion exchange with monovalent cations [21, 48]. Covalently cross-linked alginate hydrogels were fabricated to overcome this critical drawback and to better tune the mechanical properties and network parameters of the resulting gel. Generally, covalent cross-links were formed by reactions between the carboxylic groups of the alginate and bi-functional cross-linkers such as PEG-diamines. Alginate itself can be modified with functional groups such as methacrylates [65] to make a broader range of reactions available for cross-linking.

There are other interesting methods to form alginate hydrogels such as cell cross-linking and thermally-induced cross-linking. Alginate modified with cell adhesion ligand can attach to receptors on the cell membrane, forming reversible cell cross-links [66]. Semi-interpenetrating polymer network consists of linear alginate and a network of PNIPAAm cross-linked by PEG-co-PCL was prepared [67]. At higher temperature, the thermal sensitive PNIPAAm formed additional cross-links by hydrophobic interaction. This introduced 'smartness' into alginate hydrogels.

### 1.2.3 Alginate drug delivery systems

Calcium alginate hydrogels are porous with the diameter of the pores ranging from 5 to 200nm [46]. These pore sizes are rather large and hinders the diffusion of only the macromolecules effectively. Therefore, alginate hydrogels have been applied mainly to the encapsulation of protein and DNA therapeutics or living cells. A recent trend is to study the possibility of

alginate hydrogels as delivery vehicles for small molecule drugs, due to the development of numerous coating methods, blended ingredients, covalent cross-links, and enhanced drug-matrix interaction that retard the release of encapsulated drug.

Chitosan coated alginate hydrogels have been widely exploited in drug delivery systems. Chitosan is a polycation that consists of *β*-(1−4)-linked 2-acetamido-2-deoxy-D-glucopyranose and 2-amino-2-deoxy-D-glucopyranose [25]. Through polyelectrolyte complex formation, the surface pore sizes of the polyanionic alginate hydrogels can be effectively controlled by chitosan. A recent study revealed that the release of the antineoplastic drug 5-fluorouracil was slower in chitosan reinforced alginate microparticles than in their pure forms [68]. Similarly, other polycations such as polylysine, gelatine, or poly(ethyleneimine) (PEI) can serve as coating materials for alginate [48]. The polyelectrolyte complex formation can also be applied homogeneously throughout the gel to further strengthen it and eliminate the chance of catastrophic disruption should the coating layer fail [48].

Materials blended with alginate can affect the properties and drug release profile of the hydrogel. Alginate microspheres filled with carbon nanotube have been reported to have longer preserving time in the release medium, higher encapsulation efficiency, lower drug leakage and more prolonged drug release than pure alginate microsphere [69]. On the other hand, the drug release rate was increased with the increasing ratio of starch blended into alginate fibres [70].

In fact, drug release is a sophisticated process controlled by numerous factors. The hydrophilicity or hydrophobicity of the drug affects its diffusivity in the swollen matrix [71]. The ionic attraction between oppositely charged drug molecules and the hydrogel can restrict the drug release unless excess ions are added to screen the ionic interaction [72]. On the contrary, ionic repulsion between drugs and hydrogels carrying the same charge makes drug loading difficult and the subsequent release much faster. Moreover, pH, temperature and ionic strength of the release medium can all affect the swelling degree or the degradation rate of hydrogel and hydrogel-drug linkage, thus have an impact on the drug release profile.

## 1.3 Albendazole

Albendazole (ABZ), methyl 5-propylthio-1H-benzimidazole-2-yl carbamate (Figure 1.4), is a member of the benzimidazole family that has a broad spectrum of activity on human and animal helminth parasites [73, 74]. Having been applied clinically as anthelmintic drug for almost thirty years, its efficacy and safety is well recognized [75]. More recently, the potential

of ABZ as an anti-cancer drug is reported [73, 75-77]. Pourgholami et al. showed that ABZ had significant activity against a number of cancer cell lines by arresting cells in the $G_2$/M phase of the cell cycle and inducing apoptosis [76, 77]. Profound inhibition of vascular endothelial growth factor (VEGF) secretion by ABZ was also observed, abolishing tumor angiogenesis and malignant ascites formation [75].

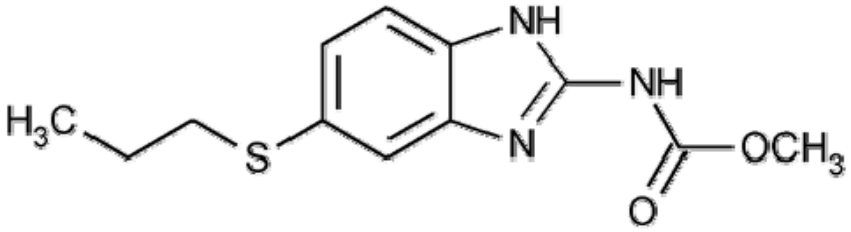


**Figure 1.4 Chemical structure of albendazole (ABZ).**

Despite its potential in the said applications, the clinical usefulness of ABZ is hampered by its very low water solubility (0.2µg/ml) [73]and *in vivo* metabolism. For systemic treatment, ABZ can only be administered orally, because its low solubility rejects the possibility of intravenous injection. When orally administered, it has limited and variable absorption and suffers from high hepatic first-pass effects. Therefore, very little drug can reach systemic circulation [76]. The major metabolites of ABZ are albendazole sulfoxide (ABZ-SO) and albendazole sulfone (ABZ-SO2), as shown in Figure 1.5. There are also a number of other metabolites, making only trace amounts of the parent drug detectable. This is due to the rapid oxidation of ABZ in the liver [74, 77]. While albendazole sulfoxide is the active metabolite responsible for the anthelmintic activity [74, 77], it was approximately 20-fold less cytotoxic than albendazole and albendazole sulfone was completely inactive in this regard [77]. Furthermore, drug formulation flexibility is significantly reduced because of the low solubility of albendazole.

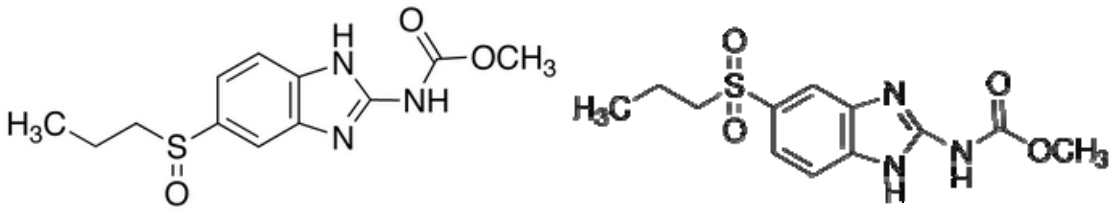


**Figure 1.5 Metabolites of albendazole: albendazole sulfoxide (left) and albendazole sulfone (right).**

An important property of ABZ that is relevant to this study is that it protonates at acidic pH. There are two tautomers of the conjugate acid formed by protonation, as shown in Figure 1.6.

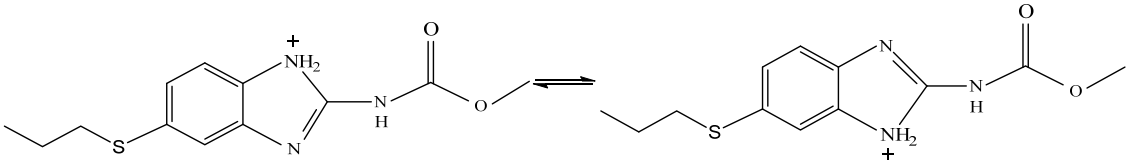

**Figure 1.6 Protonation of albendazole and the tautomers of the conjugate acid.**

In conclusion, while the low absorption rate and high hepatic clearance of albendazole may be desirable for localized and prolonged treatment [77], it is important to increase its solubility and protect it from oxidation if albendazole is to be applied for systemic cancer treatment.

## 1.4 Cucurbit[*n*]uril

Cucurbit[*n*]uril (abbreviated as Q[*n*] hereafter, where *n* stands for the number of repeating units) are a family of macrocyclic host molecules. Although first reported as the acid-catalysed condensation product of glycoluril and formaldehyde in 1905 [78], the Q[*n*] family did not receive substantial attention until the full characterization of the parent compound Q[6] in 1981 by Mock et al [79]. It was determined to be a macrocyclic glycoluril hexamer with double methylene bridges between neighbouring units. Subsequently, larger and smaller homologues which consist of different numbers of glycoluril units have been synthesized and characterized. Nowadays, the Q[*n*] family comprises Q[5], Q[6], Q[7], Q[8], and Q[10], as shown in Figure 1.7. Q[*n*] with the hydrogen atoms of the glycoluril unit partially or fully substituted have also been synthesized, as depicted in Figure 1.8. Fully substituted Q[*n*] have been synthesized by condensation of functionalized glycoluril with formaldehyde (Route a in Figure 1.8). Alternatively, they can be obtained by direct oxidation of formed Q[*n*] using potassium persulphate (Route c in Figure 1.8)[80]. Day et al. reported a method to synthesize partially substituted Q[*n*] [81]. Under acid catalysis, the mixture of glycoluril and the diether of dimethylglycoluril formed partially substituted Q[*n*] with substantial proportions being the higher homologues (*n*=6 and 7). Using this method (Route b in Figure 1.8), a symmetrical tetrasubstituted cucurbit[6]uril has been synthesized with the glycoluril replaced by its dimer [82].

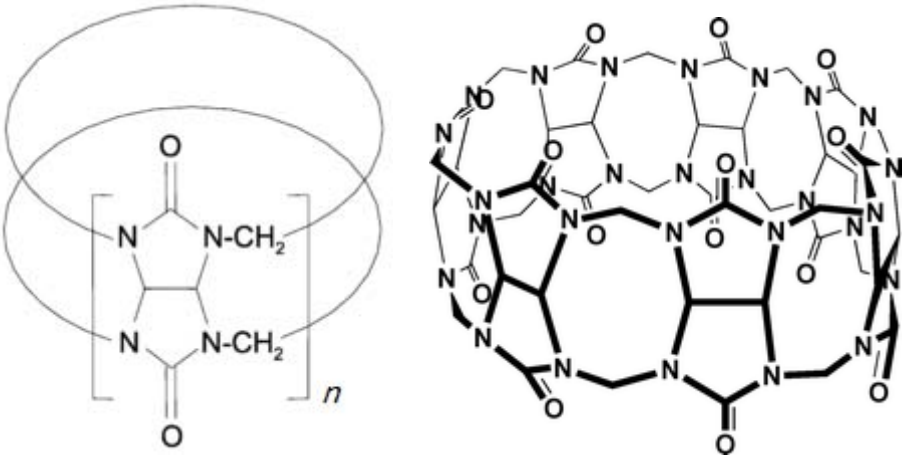

**Figure 1.7 Schematic illustration of cucurbit[*n*]uril (left, *n*=5-8 and 10) and structure of cucurbit[7]uril (right).**

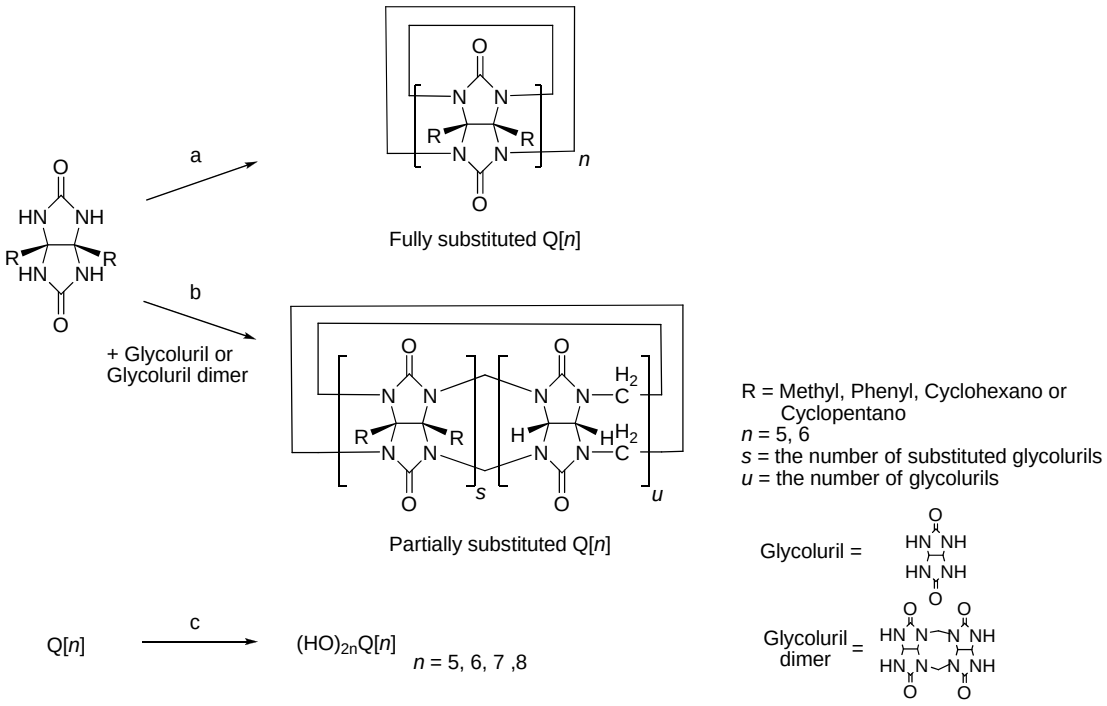


**Figure 1.8 Synthesize methods and structure of fully and partially substituted Q[*n*].**

As a member of the macrocyclic host molecules, cucurbit[*n*]uril can encapsulate other molecules in their cavity by non-covalent interactions, forming host-guest complexes, thereby modifying the properties of the guest molecules and even themselves. This kind of host-guest interaction is an important part of the broader field of supramolecular chemistry [83], and has had great impact on drug delivery. The benefits include enhanced solubility and stability of drug molecules [84].

The suitability and effectiveness of a guest to be encapsulated in a macrocyclic host highly depend on their compatibility in size, shape, polarity, and hydrophilicity [85]. Therefore, it is

beneficial to first have a look at such properties of the host of interest, cucurbit[*n*]uril, before discussing their host-guest chemistry.

### 1.4.1 Properties of cucurbit[*n*]uril

#### 1.4.1.1 Dimensions

Cucurbit[*n*]uril are barrel shaped molecules with a hydrophobic cavity that is accessible on both sides through the carbonyl oxygen rimmed portals. As can be deduced from the structure, all cucurbit[*n*]uril homologues have the same depth, while the diameter of their portals and the diameter and volume of their cavities vary systematically with ring size [86]. It is interesting to note that some derivatives of Q[*n*], such as the ellipsoid tetramethylcucurbit[6]uril [82], may have irregular cross-sections. Table 1.2 lists the dimensions of cucurbit[*n*]uril and cyclodextrins (CD). The similarity in dimensions of Q[*n*] and cyclodextrins have led to constant comparison between them.

**Table 1.2 Dimensions and properties of cucurbit[*n*]uril and cyclodextrins. Values obtained from [86] and [80].**

| | Portal diameter (Å) | Cavity diameter (Å) | Depth (Å) | Cavity volume (Å$^3$) | Solubility in water (mM) | p$K_a$ |
|---|---|---|---|---|---|---|
| Q[5] | 2.4 | 4.4 | 9.1 | 82 | 20-30 | – |
| Q[6] | 3.9 | 5.8 | 9.1 | 164 | 0.018 | 3.02 |
| Q[7] | 5.4 | 7.3 | 9.1 | 279 | 20-30 | – |
| Q[8] | 6.9 | 8.8 | 9.1 | 479 | <0.01 | – |
| Q[10] | 9.0-11.0 | 10.7-12.6 | 9.1 | 870 | – | – |
| α-CD | 4.7 | 5.3 | 7.9 | 174 | 149 | 12.332 |
| β-CD | 6.0 | 6.5 | 7.9 | 262 | 16 | 12.202 |
| γ-CD | 7.5 | 8.3 | 7.9 | 427 | 178 | 12.081 |

#### 1.4.1.2 Solubility and acidity

Cucurbit[*n*]uril have limited solubility in water and organic solvents [80]. While Q[5] and Q[7] possess moderate solubility, Q[6] and Q[8] are effectively insoluble [86]. All Q[*n*] homologues are weak bases because of the rings of carbonyl groups. The p$K_a$ value of Q[6] has been determined to be 3.02. The p$K_a$ value of other homologues, though not reported, should be in the close vicinity [86]. Accordingly, the solubility of Q[*n*] is increased dramatically in

concentrated aqueous acid. Their solubility can also be increased by the addition of certain salts, guest molecules and derivatization [80].

#### 1.4.1.3 Stability

The Q[*n*] family are both chemically and thermally robust [81]. Although Q[8] may degrade to smaller Q[n], Q[5-7] are stable in concentrated HCl at 100°C for at least 24hours [87]. Q[5-8] are stable at temperatures exceeding 370°C by thermal gravimetric analysis [86].

### 1.4.2 Host-guest chemistry of cucurbit[*n*]uril and their applications

All Q[*n*] homologues are highly symmetrical molecules with an equatorial symmetry plane. Similar to other macrocyclic host molecules such as cyclodextrins, calixarenes and crown ethers, cucurbit[n]uril can encapsulate various guest molecules in their hydrophobic cavity by non-covalent inclusion. The hydrophobic cavity provides a favourable domain for non-polar sections of a guest molecule. The carbonyl oxygens provide hydrogen-bonding opportunities [86, 88]. Due to the negative electrostatic potential at both portals rimmed by the carbonyl oxygens, the Q[*n*] family bind cationic guests preferentially [86]. This ion-dipole interaction strengthens the host-guest complex. Moreover, as the portals are approximately 2 Å narrower than the cavity, they exert significant steric hindrance to guest association and dissociation. Therefore, Q[*n*] generally bind guests with higher affinity and higher selectivity than other well known host molecules [86].

Numerous potential applications stem from the unique host-guest interaction of cucurbit[*n*]uril. They have potential in sewerage treatment due to their ability of binding heavy metals, aromatic substances and cationic dyes etc. Their binding to DNA lends possibility in gene transfection. They are also capable of forming several self-assembly systems such as molecular necklaces, pseudorotaxanes, polyrotaxanes, supramolecular amphiphiles, self-sorting systems, and molecular machines [86].

The application of Q[*n*] in drug delivery systems is especially promising. By Q[*n*] encapsulation, the solubility of hydrophobic drugs, which reveals itself increasingly challenging in drug formulation and delivery as hydrophobic drugs now take up the majority of newly developed drugs [84, 85], may be increased. Drugs can be protected from aerial oxidation, hydrolysis, thermal and light induced degradation, and the attacks from biomolecules in the body, through encapsulation [80, 84, 85, 88]. Moreover, controlled or targeted drug delivery mediated by Q[*n*] has been reported [85, 88]. The target specific delivery and the reduction of unintended reactions in the body effectively alleviate the systemic toxicities of drugs.

The size of Q[*n*] is a limiting factor in their applications. This is especially true in drug delivery. Q[5] and its derivatives can only encapsulate very small guests such as gas molecules and small solvent molecules. It is also possible for metal and ammonium ions bind at the portals of Q[5] along with water [80, 86, 89-91]. Q[7] is large enough to encapsulate adamantanes, positively charged aromatic compounds, and metal complexes. The roomy cavity of Q[8] allows simultaneous encapsulation of two aromatic rings [80]. As such, higher homologues of Q[*n*] are more desirable as drug encapsulating hosts. Substituted Q[*n*] may have higher solubility, enhanced selectivity towards certain drug, or other unique properties, and have been the constant focus of cucurbit[*n*]uril research.

### 1.4.3 Comparison with cyclodextrins

Cyclodextrins are cyclic oligosaccharides composed of 6-8 (α-, β-, and γ-cyclodextrins, respectively) α-1-4-linked glucose units [73, 92]. They have a hydrophobic cavity and a hydrophilic outer surface. Despite their similarity to cucurbit[*n*]uril in dimensions and the capability of forming non-covalent assemblies with guest molecules, the differences between cyclodextrins and Q[*n*] are quite pronounced. First of all, cyclodextrins are cone-shaped chiral molecules that have portals of different diameters on a single molecule, whereas the portals of a single Q[*n*] are identical (Figure 1.9). Secondly, cyclodextrins have a more positive electrostatic potential than Q[*n*], especially at the portals [86]. Consequently, they exhibit favourable binding to neutral or anionic guests, contrary to Q[*n*]. Lastly, cyclodextrins are less thermally stable than Q[*n*] but generally have higher solubility in water [86].

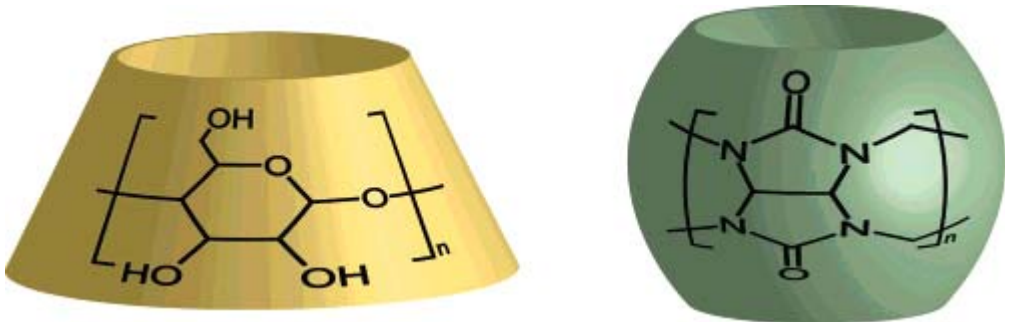


**Figure 1.9 Structural comparison between cyclodextrins (left) and cucurbit[*n*]uril (right). Figure taken from [93].**

Cyclodextrins and their derivatives are commercially available and have been studied for the delivery of hydrophobic drugs since the 1950s [85]. Release characteristics of cyclosporine encapsulated in cyclodextirn from sterilized PEG hydrogels were better than those loaded by the conventional method [92]. Complexation of albendazole with hydroxypropyl-β-cyclodextrin resulted in a 10,000-fold increase in aqueous solubility. Significantly greater antitumor activity, higher concentration and longer duration in plasma than the conventional

albendazole/hydroxypropyl methyl cellulose suspension were observed [73]. The same inclusion complex also exhibited enhanced anti-proliferative efficacy than ethanol solution of albendazole [76]. However, a major drawback of cyclodextrins as components of drug delivery systems is their toxicity [92, 94]. An exploratory study on the toxicity of Q[7] and Q[8], on the other hand, suggested that they are essentially nontoxic at concentrations far above that required for drug delivery applications [95].

## 1.5 Aims of study

A daunting challenge for hydrogel drug delivery systems is the inherent incompatibility of the hydrophilic network and hydrophobic drugs, which are sparingly soluble in both the media and the hydrogel phases. For example, Li et al. reported albendazole release from alginate-chitosan beads [74]. Only around 10% of the ABZ available was incorporated into the beads. The most common approach to resolve this problem is to introduce hydrophobic domains in the hydrophilic network [8]. However, this approach addresses only one aspect of the two-fold problem of hydrophobic drug delivery by hydrogels, i.e., the incorporation of hydrophobic molecules in hydrophilic matrices. Release of the drug into the aqueous environment remains problematic. In addition, such modifications significantly restrict hydrogel swelling and potentially reduce their biocompatibility. Alternatively, more complex systems such as drug-entrapping liposomes, microparticles, or surfactant-stabilized emulsion incorporated in hydrogels have been reported [8]. The application of macrocyclic host molecules can reduce the complexity of such combined drug delivery systems and facilitate their fabrication.

The interaction of Q[6-8] with benzimidazole derivatives was reported by Xue and co-workers [96]. Albendazole has been successfully encapsulated in Q[7] and Q[8] and its solubility was found to be drastically increased [80]. As mentioned above, albendazole protonates in acidic environments. Q[*n*] are thus superior to cyclodextrins in the encapsulation of ABZ as they have much higher association constants to protonated ABZ than cyclodetrins. In fact, the required concentration of Q[7] is more than 6-fold less than β-cyclodextrin to achieve the same solubility of albendazole [95], reducing the potential for toxic effects, if they occur.

The aim of the present study is to investigate the possibility and suitability of controlled release of albendazole from an alginate hydrogel through cucurbit[*n*]uril encapsulation. A novel cross-linking method of the alginate hydrogel is also utilized. The release of ABZ from such a combined delivery system is studied in different media. Mathematical models are subsequently applied to the release data in an attempt to identify the controlling mechanism of drug release.

# Chapter 2 Experimental results and discussion

## 2.1 Experimental

### 2.1.1 Materials

Albendazole and sodium alginate (medium viscosity) were purchased from Sigma. According to the manufacturer, the alginate is composed of approximately 61% mannuronic and 39% guluronic acid or a M/G ratio of 1.56, with molecular weight ranging from 80,000 to 120,000. $D_2O$ was obtained from Cambridge Isotope Laboratories. Glycoluril and 35wt.% DCl/ $D_2O$ were from Aldrich. Paraformaldehyde was purchased from Lancaster Synthesis. Q[7] was provided by Dr. Anthony Day, synthesized by a previously described method [87]. Milli-Q water was from a Millipore four-stage water purification unit. Other chemicals and solvents were analytical grade. All chemicals and solvents were used as received. Nylon syringe filters with a mesh size of 0.45μm were used.

### 2.1.2 Instrumental methods

One-dimensional $^1$H NMR spectra were recorded at 25°C using a Varian Unity*plus*-400 spectrometer operating at 400MHz. $^1$H NMR spectra were referenced using the residual $^1$H signal of the deuterated solvent. Between 64 to 128 transients were run for each spectrum. The spectra were analysed with Varian's VNMR software.

UV spectroscopy was performed on a Cary 50 Bio UV/Vis spectrometer, scanning from 200-400nm.

Elemental analyses were performed by the Australian National University Microanalytical Service.

### 2.1.3 Synthesis of Q[5] and Q[8]

Q[5] was synthesized according to published methods [97], with sodium cation as the template. Q[8] was isolated from the by-product of the Q[5] synthesis.

Glycoluril (30g, 0.21mol) and sodium chloride (6.17g, 0.105mol) were dissolved in 32% HCl (168ml). Paraformaldehyde (13.32g, 0.44mol equivalent) was then added. The mixture was stirred at room temperature for 30 minutes until a translucent gel was formed. This was refluxed at 90-100°C for 3 hours. The acid was removed with reduced pressure. Water (100ml)

was added to the residue and the mixture was neutralized with solid $NaHCO_3$. A white solid formed after boiling and cooling the mixture to 5°C and this was collected by filtration.

This material was dissolved in hot 32% HCl (50ml) and a hot solution of 5% aqueous $NH_4Cl$ (200ml) was added. The mixture was filtered after brief boiling and subsequent cooling to 5°C, to coarsely separate Q[5](in the filtrate) and Q[8](in the residue). The filtrate and residue ("solid-1" for Q[8] isolation) were collected separately.

*Isolation of Q[5]*

The filtrate was concentrated with reduced pressure. Water (100ml) was added to the residue, followed by addition of solid NaOH until pH was raised above 7 to precipitate a white solid. After cooling to 5°C, a crude Q[5] sodium salt was collected by filtration and washed thoroughly with sodium hydroxide solution followed by water. This step separated Q[5] from other homologues as it has a much smaller solubility in the basic NaOH solution.

The crude material was recrystallised with 16% HCl to give pure Q[5] sodium salt. Desiccating the product yielded Q[5] 6g, 14%.

*Isolation of Q[8]*

Q[8] was isolated by washing "solid-1" with formic acid because Q[8] has a very low solubility in it. "solid-1" (10g) was suspended in 60% formic acid (100ml, "solid-1" to formic acid ratio, 1:10 w/v). The suspension was centrifuged for 1 hour and supernatant was decanted. The residue was washed with 60% formic acid (50ml) again followed by washing with water, using the said procedure. Desiccation of the residue yielded Q[8] 3g, 7%.

Purity of the synthesized Q[5] and Q[8] was confirmed by $^1H$ NMR with the addition of authentic Q[5] and Q[8]. Both NMR samples were prepared with 35% $DCl/D_2O$.

It has been demonstrated that alkali and alkaline earth cations form 1:1 or 2:1 complexes with Q[6] in aqueous solution by binding at the carbonyl oxygen rimmed portals [89-91], and that this is generally true for the Q[*n*] family [86]. The solubilities of Q[*n*] can be increased by the formation of such complexes. It is hence useful to determine the solubility of the synthesized Q[5] sodium salt.

To prepare saturated Q[5] solutions, excess Q[5] sodium salt was added to Milli-Q water or pH3 water (using diluted HCl). The mixture was heated to 80°C and cooled to room temperature. Filtering with a syringe filter gave the saturated Q[5] solutions. The solubility of

the Q[5] sodium salt in water and pH3 water was determined by completely drying 2.00mL of respective saturated solution on a evaporating dish. The resulting solubilities of Q[5] at room temperature were 26.0g/L in water and 21.1g/L in pH3 water, respectively.

### 2.1.4 Preparation of the albendazole-Q[*n*] complex

#### 2.1.4.1 Procedures

Albendazole was encapsulated in Q[7] and Q[8] according to the documented method [80]. Briefly, albendazole and solid Q[*n*] (*n*=7, 8) were mixed in pH3 Milli-Q water. The mixture was homogenized using a vortex shaker, sonicated for 1.5 hours and then left to stand overnight at room temperature. The mixture was then filtered through 0.45μm syringe filter to give clear solutions of ABZ@Q[*n*] complex, which was freeze-dried to give solid product.

#### 2.1.4.2 Characterization

Weight percentage of albendazole in the ABZ@Q[*n*] complex and the molar ratio of ABZ:Q[*n*] were determined by $^{1}$H NMR. The spin-lattice (T1) relaxation time of the pulse sequence was adjusted to ensure all $^{1}$H nuclei were relaxed before the onset of the next transient. An accurately weighed amount of the complex was dissolved in $D_2O$, and 10μL of standardised tertiary butanol/$D_2O$ solution (0.0104mol/L) was added. The amount of albendazole was obtained by comparing peak area integrals of selected peaks of ABZ and the peak of tertiary butanol, using equation (2.1). Similarly, the molar ratio of ABZ:Q[*n*] was calculated from peak area integrals of selected peaks of ABZ and Q[*n*].

$$n_{ABZ} = \frac{n_{TB} P_{TB} A_{ABZ}}{P_{ABZ} A_{TB}} \qquad (2.1)$$

Here, $n_X$ = the amount of substance X; $P_X$ = the number of protons of the selected peaks, and $A_X$ = the peak area integral. Subscripts *ABZ* and *TB* stand for albendazole and tertiary butanol, respectively.

The amounts of ABZ, Q[*n*] and water used for the preparation of ABZ@Q[7] and ABZ@Q[8] are listed in Table 2.1, along with the characterized properties of the ABZ@ Q[*n*] complexes.

**Table 2.1 Amount of materials used, yield, and the characterized properties of the dry ABZ@Q[*n*] complexes.**

| | Amount of materials used | | | Properties of the dry complexes | | |
|---|---|---|---|---|---|---|
| | Albendazole | Q[*n*] | Milli-Q water | Yield | ABZ:Q[*n*] Solution Ratio | ABZ Weight Percentage |
| ABZ@Q[7] | 180.4mg, 0.68mM | Q[7] 473mg, 0.41mM | 45ml | 476.3mg, 73% | 0.55 | 11.05% |
| ABZ@Q[8] | 40mg, 0.15mM | Q[8] 199.2mg, 0.15mM | 50ml | 189mg, 79% | 0.88 | 14.45% |

### 2.1.5 Determination of the extinction coefficients

The extinction coefficients of the ABZ@Q[*n*] complex in different media were determined by the UV spectrophotometric method. The concentration range of ABZ used was based on the reported linearity range and limit of quantification [98].

An accurately weighed amount of the ABZ@Q[*n*] complex was dissolved in 3ml water, pH3 water, pH3 0.5M NaCl solution and pH1 water to yield equivalent ABZ concentrations, c.a. 20μg/mL. The solutions were diluted by half with respective medium for five times, yielding a final concentration c.a. 0.625μg/mL. UV spectra were recorded for the original solutions and after each dilution. Absorption maxima (nm) were determined from the six spectra of each sample (Table 2.2). Absorbance at the maximum was plotted against concentration. A linear equation was fitted for each plot and the slope, intercept, and coefficient of correlation were recorded, as listed in Table 2.2. Extinction coefficients are the slopes of the fitted linear equations.

**Table 2.2 Absorption maxima, extinction coefficients and statistical parameters of the ABZ@Q[*n*] complexes in different media.**

| Drug complex | Medium | Absorption maximum (nm) | Extinction coefficient ($\varepsilon$) | Intercept | Coefficient of correlation ($R^2$) |
|---|---|---|---|---|---|
| ABZ@Q[7] | Water | 296 | $1.1\times10^4$ | 0.048 | 0.9989 |
| | pH3 Water | 294 | $1.2\times10^4$ | 0.0016 | 0.9995 |
| | pH3 0.5M NaCl | 293 | $1.3\times10^4$ | 0.0112 | 0.9989 |
| ABZ@Q[8] | Water | 302 | $1.1\times10^4$ | 0.0076 | 0.9999 |
| | pH3 Water | 292 | $1.0\times10^4$ | $-9\times10^{-6}$ | 1 |
| | pH3 0.5M NaCl[a] | 294 | $8.6\times10^3$ | 0.0091 | 0.9999 |
| | pH1 Water[a] | 292 | $7.3\times10^3$ | 0.0102 | 0.9999 |

a. Resulted in a milky mixture when ABZ@Q[8] concentration was high (20μg/ml equivalent ABZ). The mixture became clear after dilution.

All data points agreed well with the fitted linear calibration curves, as indicated by the coefficient of correlation. The presence of NaCl did not have a significant effect on the absorption maximum while more acidic pH caused a blue shift, especially for the ABZ@Q[8] complex. The more significant blue shift of ABZ@Q[8] in acidic environment as compared to ABZ@Q[7] may be due to different binding orientations of ABZ facilitated by the larger cavity of Q[8]. At the upper end of the concentration range studied for ABZ@Q[8], the presence of 0.5M NaCl or a pH1 solution led to a milky mixture, which is probably the result of competitive binding of the sodium ion and $H^+$ to Q[8]. Such competitive binding has been evidenced by the decreased binding constant between the 4-methylbenzylammonium guest and the Q[6] host when a simple salt was introduced to the solution [89]. The baseline was shifted in such cases and the extinction coefficients are significantly lower. The respective calibration curves are thus invalid. As NaCl had little effect on the absorption maximum and its value at pH1 is identical to that at pH3, and the drug complex concentrations in the release studies were much lower (where the above distortion was not observed), conversions from absorbance to drug concentration in such media were carried out according to the calibration curve of ABZ@Q[8] in pH3 water.

### 2.1.6 Preparation of the Q[5] alginate hydrogel beads

#### 2.1.6.1 Preparation of saturated Q[5] solution

Saturated Q[5] solutions were used for the gelation of alginate beads. These are prepared with water and pH1 water, as described in section 2.1.3.

#### 2.1.6.2 Preparation of alginate beads

Alginate hydrogel beads were prepared in two different ways.

*Method A*

Sodium alginate solution (2% w/v) was prepared and left to stand overnight to remove air bubbles. This precursor solution was dripped from a plastic pipette into saturated pH1 Q[5] solution to form beads. The pipette tip was held 5cm above the surface of the gelling solution to facilitate the formation of spherical beads. The beads were left in the solution for 30 minutes under gentle stirring, washed with water and dabbed dry with filter paper.

*Method B*

Sodium alginate powder was dissolved in saturated Q[5] solution (2% w/v) and stirred overnight. This precursor solution was dripped into pH1 water and gelled in the same manner as *Method A*. The weights of the precursor solution used and the formed beads were recorded for each preparation.

#### 2.1.6.3 Drug loading

Two methods were used to load the drug complexes into the alginate beads for drug release studies. The first method was applied to the beads prepared by both of the gelling methods in section 2.1.6.2. The second method was used only for the beads prepared by *Method B*.

(1) Weighed amounts of the ABZ@Q[*n*] complex were dissolved in the precursor solution of *Method A* or *B* before gelation, making precursor solutions of different formulations which will be given in Table 2.5. All the drug loaded beads were prepared according to this method unless otherwise stated.

(2) Empty beads prepared by *Method B* were immersed in solutions of the drug complexes and left to reach equilibrium, washed with water and dabbed dry with filter paper. In all cases, this was carried out in UV cells containing 3ml of drug complex solution and 3 empty beads, with gentle stirring. Absorbance in the supernatant was monitored at respective absorption maximum until equilibrium was reached and was converted to drug concentration, using the calibration curves obtained in section 2.1.5.

The amount of drug loaded into the beads was calculated from the initial concentration and the final equilibrium concentration.

The rate and amount of drug complex uptake by the empty beads also provide valuable information on the interactions between the drug complexes and the Q[5] alginate hydrogel. Concentrations of ABZ at different time intervals were normalized against the initial concentration. All such drug uptake experiments were conducted in triplicate and presented as mean values ± standard deviation.

#### 2.1.6.4 Determination of drug loading content and drug loading efficiency

Drug loading content (%) is the weight percentage of the loaded drug relative to the dry weight of drug-loaded hydrogel. Drug loading efficiency (%) indicates how much of the drug supplied is effectively loaded. Determining the amount of the effective drug in a certain amount of hydrogel prepared is the prerequisite for the calculation of both.

Different formulations of hydrogel beads as used for the drug release studies were prepared, freeze-dried and pulverized. Their weights just after gelation and after freeze-drying were recorded. UV spectroscopy was used to determine the mass of ABZ in such dry samples.

An accurately weighed dry sample (c.a. 4mg) was dissolved in 3.9mL physiological saline with the addition of sodium bicarbonate to slightly raise the pH. Subsequently, 0.1mL of 0.1M HCl was added to the solution. The resulting mixture was filtered by syringe filter to give a clear solution. The concentration of ABZ was determined by UV spectroscopy using the calibration curves obtained in section 2.1.5. The amount of ABZ with respect to the dry samples was then calculated.

Drug loading content and drug loading efficiency of beads made from each precursor solution formulation can be calculated with the knowledge of the formulation of the precursor solution, the weight of the precursor solution used to obtain a certain amount of dry sample, and the amount of ABZ in the dry sample.

### 2.1.7 Media used in this study

The media used for elemental analysis of alginate beads, swelling tests and drug release studies are listed in Table 2.3. All media were prepared with Milli-Q water. Buffer solutions were not used in order to avoid the complication of introducing other ions. The terms water, aqueous NaCl etc. are used throughout the thesis to always refer to the pH and salt concentrations as described in Table 2.3.

**Table 2.3 Media used in this study.**

| Name of medium | pH* | NaCl concentration (mol/L) |
|---|---|---|
| Water | 6.3 | 0 |
| Aqueous NaCl | 6.3 | 0.5 |
| pH3 Water | 3 | 0 |
| pH3 NaCl | 3 | 0.5 |
| pH1 Water | 1 | 0 |
| pH1 NaCl | 1 | 0.5 |
| Physiological saline | 6.3 | ~0.154 |

*As measured using a pH meter.

### 2.1.8 Elemental analysis of empty alginate beads

Empty alginate beads prepared according to *Method B* were immersed in 200mL of water and 200mL of 0.5M NaCl at pH3, with gentle stirring. After 1 hour, 3 hours and 1 day, the beads were taken out, washed with water and desiccated in an oven at 80°C. Weight percentages of the elements C, H, N, Na, and Cl in the samples were determined by elemental analysis.

### 2.1.9 Swelling tests of empty alginate beads

Ideally, swelling ratios (SR) of hydrogels should be the weight ratio of the fluid absorbed by a hydrogel sample and its dry weight, as given by equation (2.2), where $W_s$ is the weight of the hydrogel in the swollen state and $W_d$ is the dry weight of the hydrogel.

$$SR = \left(W_s - W_d\right) / W_d \qquad (2.2)$$

However, as the alginate beads prepared in this study do not rehydrate very well after freeze-drying, the dry weights of the swollen hydrogels had to be calculated using a ratio of the weight of the hydrogel right after gelation and its dry weight after freeze-drying, obtained from samples separately prepared. This is considered valid because this ratio is fairly constant at 3.07±0.04%. Moreover, as the hydrogel beads used for drug release studies were not freeze-dried before use, the swelling ratios thus obtained are at least accurate for comparisons within this study.

Beads prepared according to *Method B* were dabbed with filter paper and accurately weighed after gelation. They were subsequently put in the media as listed in Table 2.3 with gentle stirring. The beads were taken out at certain time intervals, dabbed with filter paper, weighed

and put back into the respective swelling media. The swelling ratios were calculated using equation (2.2).

### 2.1.10 Drug release studies

All the hydrogel swelling, drug uptake and drug release studies were conducted at ambient temperature. Although the temperature was not precisely controlled in the drug release studies, they were conducted in parallel times of a day and should be valid for comparison within this work.

It is worth noting that ABZ remained encapsulated in the Q[*n*] during the whole process from drug loading to release, because of its relatively high binding constants with Q[7] and Q[8], which are at least at a magnitude of $10^8$ $M^{-1}$ according to the calculation based on the increase of solubility before and after encapsulation [80].

*Drug release from the beads loaded by the first method*

For drug-loaded beads made according to *Method A*, three of them were put into a UV cell containing 3mL of aqueous NaCl with gentle stirring. At certain time intervals, the drug concentration in the release medium was determined by UV at the absorption maximum, using the calibration curve of pH3 NaCl, as given in Table 2.2. This is because the pH decreased to ~3 soon after the experiments started, as the beads were gelled in a pH1 solution and alginate has a p$K_a$ of ~3.5 [99]. The amount of drug released was calculated from the determined concentrations.

To better maintain the properties of the release media and to closely mimic "perfect sink" conditions, the following method was adopted.

For drug-loaded beads made according to *Method B*, 6 beads were put into a vial containing 6mL of release medium with gentle stirring. At certain time intervals, 2mL of the release medium was withdrawn and replaced by fresh medium. The drug concentration in the medium withdrawn was determined. The cumulative amount of drug released at each time interval can be calculated using the following equation.

$$M_t = C_n \times 6 + \sum \left( C_1 + C_2 + \ldots + C_{n-1} \right) \times 2 \qquad (2.3)$$

Here, $M_t$ is the cumulative amount of drug released at each time interval and $C_n$ is the determined drug concentration in the medium withdrawn in mol/mL. *n* is the number of sampling.

The percentage of drug released (amount of drug released over time relative to the total amount of drug in the beads) was plotted against time. For these drug release studies, each experiment was conducted in triplicate and presented as mean values ± standard deviation.

To determine the total amount of ABZ in the beads prepared according to *Method A*, sodium bicarbonate was added to the UV cell at the end of each experiment. This raised the pH to above 7, which dissolved the beads. The solution was adjusted back to ~pH3 with diluted HCl (particles were observed in the mixture). The total amount of drug that was in the beads was determined by UV spectroscopy after filtering this mixture with syringe filter.

The total amount of ABZ that was in the beads prepared according to *Method B* can be calculated with the knowledge of the amount of precursor solution used, the formulation of the precursor solution, and respective drug loading efficiency.

*Drug release from the beads loaded by the second method*

For beads loaded by soaking in drug complex solutions, the total amount of ABZ in the beads were determined as described in section 2.1.6.3. Beads from the triplicates of one drug uptake experiment were washed with water and put into a conical flask containing 10mL of release medium with gentle stirring. At certain time intervals, 3mL of the release medium was withdrawn and replaced by fresh medium. The drug concentration in the medium withdrawn was determined and the cumulative amount of drug released at each time interval was calculated using equation (2.3), with the constants changed to 10 and 3, respectively. The results are presented as percentage of drug released against time.

## 2.2 Results and discussion

### 2.2.1 Time-dependent composition of empty alginate beads

Weight percentages of elements present in empty alginate beads at different time intervals after immersion in different media are tabulated below.

**Table 2.4 Weight percentages of elements present in empty alginate beads at different time intervals.**

| Time | Element | Weight percentage (%) | |
|---|---|---|---|
| | | Water | pH3 0.5M NaCl |
| 1 hour | C | 35.93 | 21.93 |
| | H | 4.48 | 2.63 |
| | N | 3.67 | 0.48 |
| | Na | 0.2 | 21.87 |
| | Cl | 0.21 | 30.83 |
| 3 hours | C | 36.32 | 16.49 |
| | H | 4.79 | 1.94 |
| | N | 3.03 | 0.09 |
| | Na | 0.11 | 19.05 |
| | Cl | 0.12 | 33.71 |
| 1 day | C | 36.40 | 10.80 |
| | H | 4.92 | 1.23 |
| | N | 2.61 | 0.00 |
| | Na | 0.13 | 18.07 |
| | Cl | 0.18 | 32.31 |

The ratios of Q[5] and sodium ion relative to alginate repeating units can be calculated using the elemental analysis data and are shown as plots of the ratios against time (Figure 2.1). It should be noted that the ratios were initially identical, as the beads were prepared in one batch. The time-dependent change of the ratios was purely due to soaking the beads in different media.

The depletion of Q[5] from the beads was found to be fast in the first three hours both in water and in pH3 NaCl, as indicated by the slope of the curves (Figure 2.1 (a)). However, the depletion of Q[5] was much faster in pH3 NaCl, which led to a much lower ratio of Q[5] to alginate repeating units than in water. In fact, beads immersed in water possessed a relatively

high concentration of Q[5] after 24 hours while Q[5] was completely depleted from those immersed in pH3 NaCl. From Figure 2.1 (b), it appears that the depletion of Q[5] in pH3 NaCl was associated with a sharp increase in sodium content, while the sodium content of the beads in water was stable after three hours, accompanied by only a slight decrease in Q[5] concentration. The complete depletion of Q[5] in high salt concentration solution is consistent with the observed ion exchange of monovalent cations in the calcium alginate hydrogel [21, 48]. Considering the ability of Q[*n*] to bind cations at their portals [86, 89-91], Q[5], with sodium ions bound at its portals, probably serves to some extent as a divalent cation to assist with the cross-linking of the alginate chains.

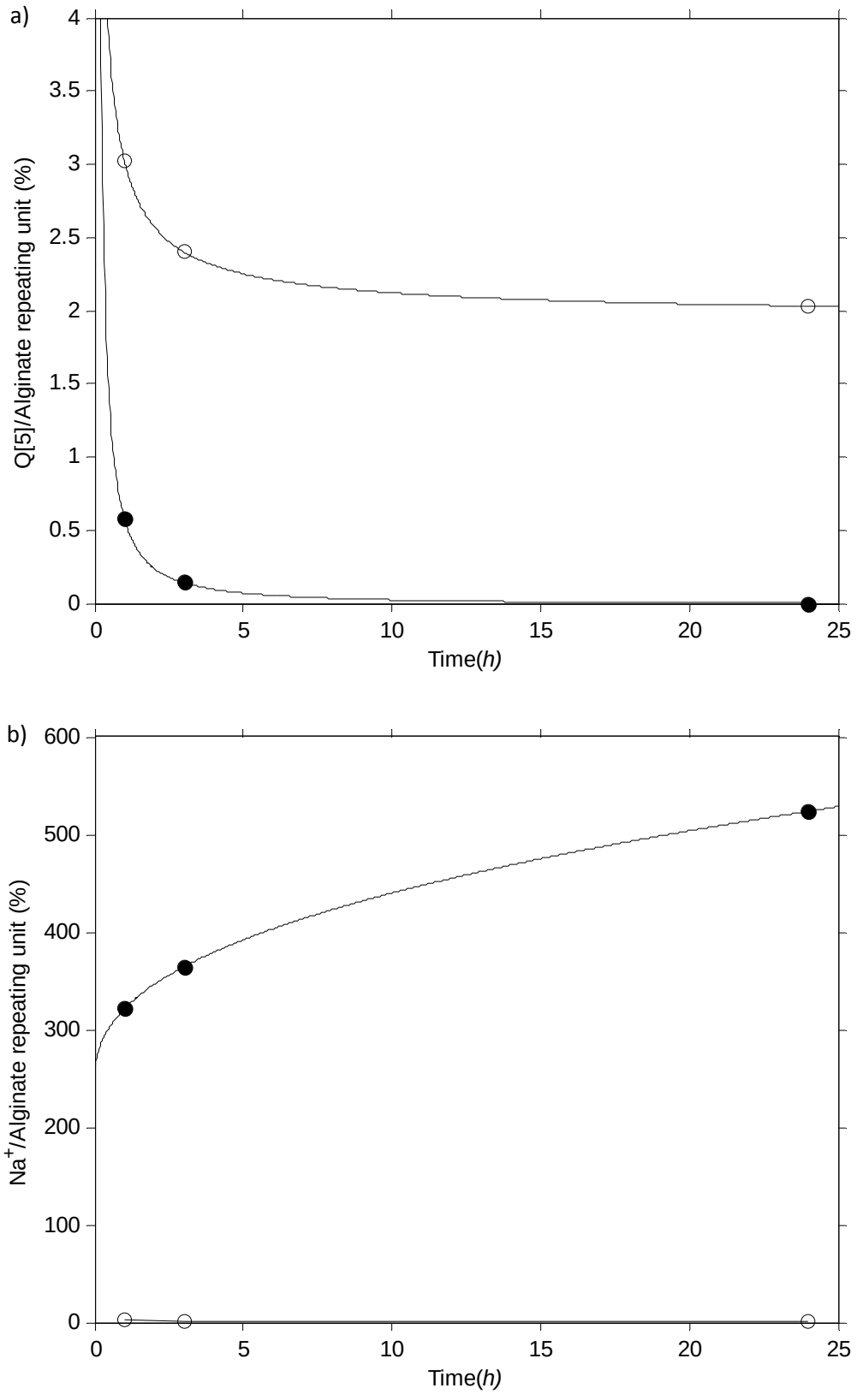


**Figure 2.1 The ratios of Q[5](a) and $Na^+$ (b) relative to alginate repeating units in water (○) and pH3 0.5M NaCl (●).**

### 2.2.2 Swelling behaviour of Q[5] alginate beads in different media

The swelling of alginate beads over time in different media is plotted in Figure 2.2. The swelling of the beads was found to be dependent on both the pH of the medium and the presence of salt.

As can be concluded from the swelling ratios in water, pH3 water and pH1 water, higher pH led to higher degree of swelling. Beads immersed in pH1 water showed a very small degree of shrinking even after the 30-minute gelling time. This pH-dependent swelling behaviour of the beads is in accordance with reported swelling studies on alginate hydrogels [74, 100, 101].

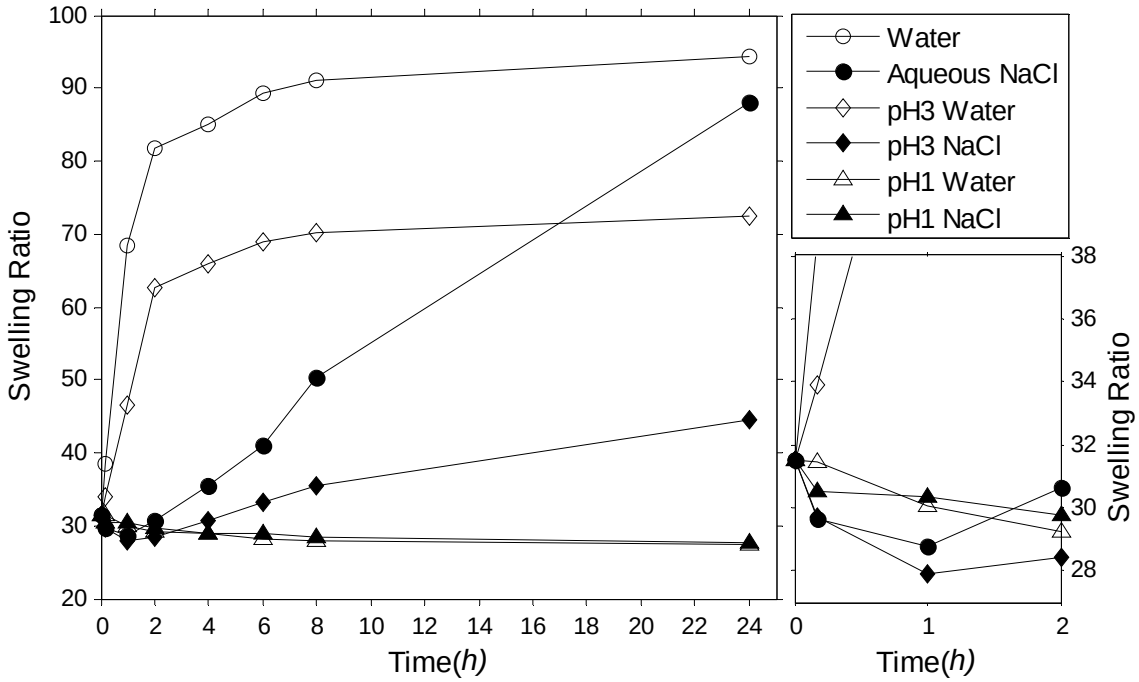


**Figure 2.2 Swelling ratios of alginate beads in different media.**

A 0.5mol/L concentration of sodium chloride in the swelling medium had considerable impact on the swelling behaviour of the beads. In aqueous NaCl and pH3 NaCl, the beads showed a weight loss (8.7% and 11.4% of the wet weight just after gelation, respectively) in the first hour, as opposed to the immediate weight increase in respective salt-free media. This could be attributed to the dissolution of the solid components and hence attenuated ability to hold fluids, rather than the shrinking of the beads due to the high osmotic pressure exerted by sodium chloride. This idea is supported by the fact that all the beads initially floated on the surface and then sank to the bottom within two minutes, which indicates that the equilibrium of salt concentration had been reached in a period much shorter than the observed weight loss. Yet more evidence is that the presence of excess salt had no impact on hydrogel swelling

at pH1. The weight loss in pH1 NaCl (3.8%) was less than those in aqueous and pH3 NaCl and its time-dependent swelling was almost identical to that in pH1 water. As alginate has a p$K_a$ of ~3.5 [99] and it can be fully protonated at pH1 to form an acid gel, the dissolution of solid components is restricted to a much lesser extent. The slight decrease in the swelling ratio in pH1 media is most probably due to the shrinking of the beads and the accompanied expulsion of water, as the beads were obviously less voluminous in such media.

After one hour, the dissolution in aqueous and pH3 NaCl became less pronounced and the swelling of the beads prevailed, leading to a gradual increase in the swelling ratio. This transition in the swelling ratio has also been observed in calcium alginate soaked in 0.1M NaCl aqueous solution and was also explained as the disintegration of alginate [48]. However, the initial weight loss lasted for six hours in the reported study [48], which was presumably due to the lower concentration of NaCl compared to this study. The final swelling ratios in both aqueous NaCl and pH3 NaCl are smaller than those in the respective salt-free swelling media, which also suggested some degree of dissolution of the solid components, especially when taking the weight of the substantial amount of sodium that condensed on the alginate chains into account. Disintegration of the beads in the presence of excess salt is further evidenced by the much weaker beads at the end of the experiments (larger deformation when handled with tweezers and deformed under its own weight), compared to their counterparts in the salt-free media. Together these observations suggest a substantial contribution of ionic cross-linking to the gelation of the beads.

It is also worth noting that the curve shapes with or without salt is very different at pH6.3 and pH3. In the salt-free media, swelling was significant in the early stage but levelled off after approximately eight hours. While for the high salt concentration media, swelling was almost linear for the period studied.

### 2.2.3 Drug release studies

The objective of this work is to achieve a substantial loading of the sparingly soluble drug ABZ into a hydrogel, through the encapsulation in Q[*n*], to provide controlled release of the drug@Q[*n*] complexes. With an understanding of our empty alginate hydrogel, it is then essential to investigate the actual performance of the combined drug delivery system and the factors that affect its release profile.

### 2.2.3.1 Formulation and properties of the drug-loaded alginate beads

The formulation of the alginate beads, along with the different release media, were designed in a way that the effects of each independent variable can be investigated. The independent variables, including the gelling method used, the formulation of the precursor solutions, the nature of the release media, and the different encapsulating Q[*n*] used, are discussed in sections 2.2.3.2 to 2.2.3.6. Formulation of the precursor solutions, the gelling method used and the drug loading properties of different kinds of alginate beads made can be found in Table 2.5.

**Table 2.5 Formulation of different precursor solutions and the properties of formed alginate beads.**

| Formulation code | Gelling method | Amount of drug supplied[a] | Drug loading content (%) | Drug loading efficiency (%) |
|---|---|---|---|---|
| 7A-low | *Method A* | 3.52mg ABZ@Q[7] | _ | _ |
| 8A-low | *Method A* | 3.52mg ABZ@Q[8] | _ | _ |
| 7B-low | *Method B* | 3.52mg ABZ@Q[7] | 0.38 | 36.97 |
| 7B-high | *Method B* | 32.23mg ABZ@Q[7] | 2.11 | 26.83 |
| 8B-low | *Method B* | 3.52mg ABZ@Q[8] | 0.73 | 47.66 |
| 8B-high | *Method B* | 9.88mg ABZ@Q[8] | 1.58 | 43.68 |

a. The amount of drug complex added is relative to 0.04g sodium alginate dissolved in 2ml of saturated Q[5] solution. The higher value of each type of ABZ@Q[*n*] complex added is calculated from the maximum solubility of that drug complex in water (~6mM for ABZ@Q[7] and ~2.7mM for ABZ@Q[8]), as reported in [80].

*Appearance of the precursor solutions and the formed beads*

The visual appearance of the precursor solutions prepared for gelling *Method A* differed considerably from those prepared for gelling *Method B*. The former (*Method A*) appeared identical to aqueous alginate solution (2% w/v), being translucent and free flowing, while the latter (*Method B*) was much more viscous and opaque with a white colour. The difference is attributed to the presence of Q[5], as alginate solutions made with pure water and saturated Q[5] solution without the drug complexes exhibited the same difference.

The presence of drug complexes also had an influence on the precursor solutions, but perceptible effects were limited to the case of 7B-high, which was less viscous than all the

other precursor solutions prepared for gelling in *Method B*. In addition, the beads formed by this precursor solution were sticky to filter paper and recovered more slowly when deformed, compared to all the other beads. The presence of ABZ@Q[8], up to its maximum concentration, did not have directly observable effects on the precursor solution.

*Verification of drug loading following bead formation*

A relatively high drug loading content and drug loading efficiency would verify that encapsulation in Q[*n*] is an effective way of overcoming the inherent incompatibility between sparingly soluble drugs and hydrogels, a major goal of this work. The first attempt to determine these parameters was by microanalysis, as sulphur should be exclusive to ABZ.

Although expected to be a more accurate method, the attempt using microanalysis was unsuccessful because 0.35wt% of sulphur was found in the alginate powder used. The results are thus unreliable as the weight percentage of sulphur introduced by the impurity is much larger than the theoretical value assuming a 100% drug loading efficiency, if the alginate was pure. The impurity in alginate may have originated from sulphate esters, as sulphuric acid could have been used during the extraction process. Alginate is derived from natural sources so that traces of sulphate containing polysaccharides such as agar and carrageenan may also remain [102].

Therefore, the values of drug loading content and efficiency listed in Table 2.5 were determined by UV spectroscopy. One sees that a relatively high loading efficiency was achieved, compared to a value of less than 10% in a study using a suspension of ABZ [74]. Although loading efficiency decreased (from ~37% to ~27% for ABZ@Q[7] and from ~48% to ~44% for ABZ@Q[8]) with increasing amounts of drug complexes supplied, this still led to a higher drug loading content (2.11wt.% for 7B-high and 1.58wt.% for 8B-high).

Drug loss during gelation can be partially attributed to the shrinking of the beads, which following gelation took up on average 80% of the weight of the precursor solution used. The drug complexes were squeezed out with water as the beads shrank. In addition, the $H^+$ ion pushed the drug complexes out of the matrix through their competitive binding to alginate, as will be discussed in sections 2.2.3.3 and 2.2.3.4. Therefore, drug loading content and efficiency would probably be higher if the same concentration of the drug complexes could be provided in the gelling solution.

ABZ@Q[8] had higher loading efficiency than ABZ@Q[7] under both drug loading amounts and its decrease in loading efficiency with increased amount of drug supplied was less pronounced. This difference between ABZ@Q[7] and ABZ@Q[8] can be explained by the higher affinity of ABZ@Q[8] to alginate and its higher ability in forming aggregates, and therefore more resistant to bead shrinking and competitive binding exerted by $H^+$. This will be discussed in section 2.2.4. On the other hand, ABZ@Q[7] achieved the highest drug loading content, due to its higher solubility in water.

#### 2.2.3.2 The effect of the gelling method on drug release

Drug release in aqueous NaCl from beads prepared by gelling *Method A* and *B* is depicted in Figure 2.3. For ABZ@Q[7] loaded beads, there is no significant difference observed for the two gelling methods, in terms of the shape of the drug release profile, or the final percentage of drug released. However, release from beads prepared by *Method A* showed some fluctuation between 3 hour and 8 hour, and the standard deviations are always larger than those of beads prepared by *Method B*.

For ABZ@Q[8] loaded beads, while the cumulative release is the same for both gelling methods, drug release from beads prepared by *Method B* was slower than from those prepared by *Method A* after 30 minutes. In addition, drug release from *Method A* beads was complete after 8 hours but lasted longer for *Method B* beads.

This could be explained by the reported observation of the heterogeneous distribution of the calcium ion in calcium alginate hydrogels formed by dripping alginate solution into aqueous $CaCl_2$ solution, which led to a polymer concentration gradient as well as inconsistency in material properties such as the pore size [44, 72]. Even the distribution of the loaded therapeutic can follow the polymer concentration profile, especially when there are considerable interactions between them [72]. As ABZ was in its protonated form, electrostatic attraction between the drug complexes and the anionic alginate is expected. Therefore, it is plausible that there were concentration gradients for both the alginate and the drug complexes from the surface to the core in the beads gelled according to *Method A*. The higher concentration of ABZ@Q[8] in the surface region and a less homogeneous gel structure in *Method A* beads then led to the faster drug release observed.

If the above discussion is a true description of the situation, then the insignificant response of ABZ@Q[7] to different gelling methods is an implication of its lower degree of interaction with alginate and smaller effective size than ABZ@Q[8], as will be further discussed in section 2.2.4.

In conclusion, gelling *Method B* ensures a homogeneous distribution of both Q[5], the likely cross-linker, and alginate. It may also have thus preserved the homogeneous distribution of the drug complexes. It is therefore more desirable than *Method A* and was used for all following studies. As a last note, the different ways of handling the drug release studies from *Method A* beads and *Method B* beads (section 2.1.10) did not have observable influences on the release profiles.

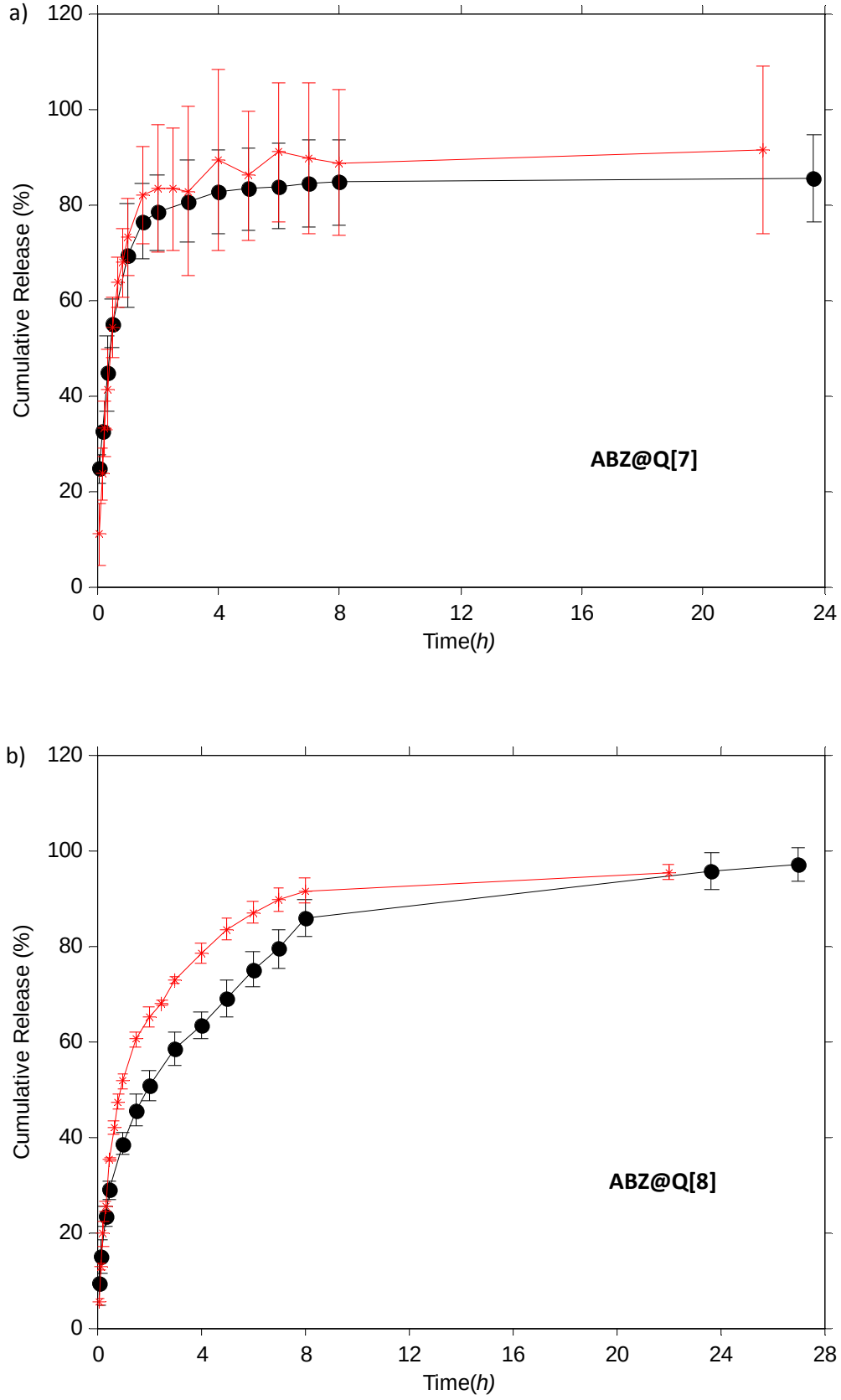


**Figure 2.3 Cumulative release of ABZ@Q[7](a) and ABZ@Q[8](b) into aqueous 0.5M NaCl solution from alginate beads prepared by gelling *Method A* (7A-low, 8A-low) (*) and *Method B* (7B-low, 8B-low) (●).**

#### 2.2.3.3 The effect of pH on drug release

The effects of different variables on the release behaviour of both ABZ@Q[7] and ABZ@Q[8] were studied. It was found that ABZ@Q[8] showed a larger response to different conditions and provided more consistent results (as indicated by its smaller standard deviation). General discussions in the following sections that are applicable to both ABZ@Q[7] and ABZ@Q[8] are based on the experimental results of ABZ@Q[8]. Differences between the two complexes will be noted and summarized in section 2.2.3.6.

Figure 2.4 shows the release profile of ABZ@Q[8] in release media at different pH. More than 80% of the loaded drug was released in pH1 water, while this value is approximately 20% and 10% for the release in pH3 water and water, respectively. In addition, the release in pH1 and pH3 water lasted for 8 hours, while the release curve in water had a very low gradient after 2 hours.

It is commonplace to relate the drug release rate or cumulative drug release with the mesh size of the hydrogel, which is indicated by the swelling ratio, as networks of larger mesh size provide less hindrance to the diffusion of the drug. The reverse, however, is observed in this study as the swelling ratios of the beads decreased significantly from water to pH3 water and pH1 water. A relative low cumulative release in water is observed not only for this formulation, it was observed regardless of the amount and type of the drug complex loaded. Alginate protonates to its acid form at lower pH with its electrostatic attraction to the cationic species reduced. The observation suggests that there is substantial interaction between the drug complexes and alginate, which restricts the effective release of the drug complexes. Under such cases, the effect of the swelling ratio on drug release was masked by the strong drug-hydrogel interaction. This interaction is further evidenced in the next section where the effect of excess salt is revealed. The very high cumulative release in pH1 water partially explains the drug loss during gelation (more than 50%, section 2.2.3.1).

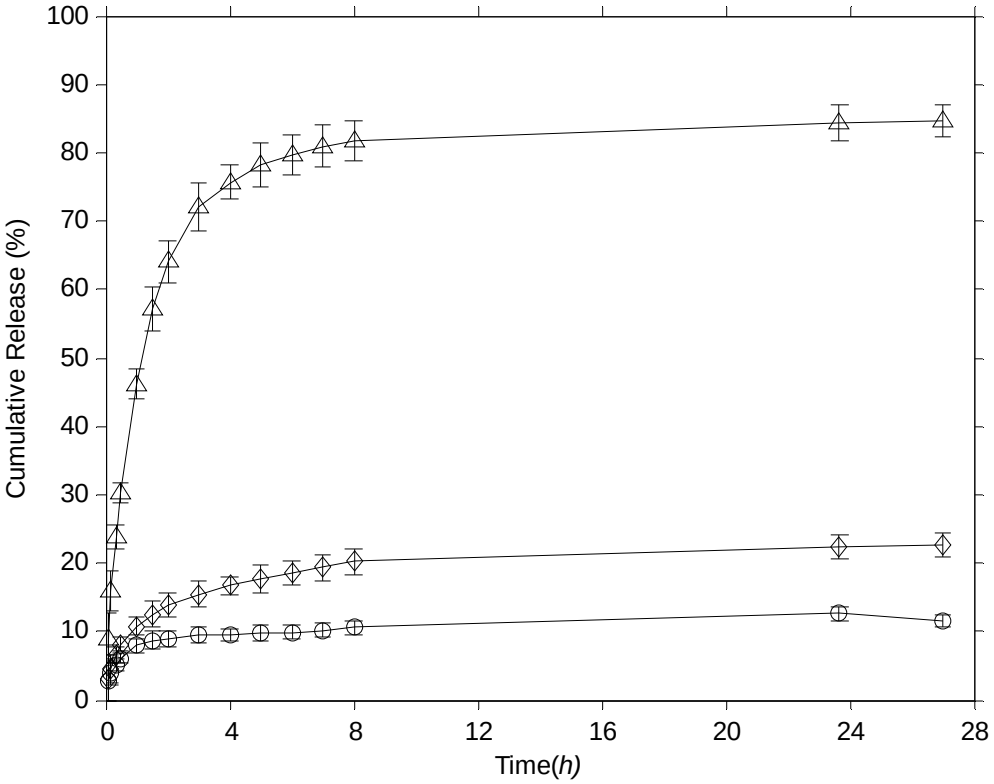


**Figure 2.4 Release of ABZ@Q[8] (8B-high) in release media of water (○), pH3 water (◇) and pH1 water (△).**

### 2.2.3.4 The effect of excess salt on drug release at different pH

As a means to understanding the drug release mechanism, it is interesting to investigate if the presence of excess salt, whose cations will compete with the drug complexes for the binding to alginate, can "free" the drug complexes and enable substantial release at near-neutral pH. In addition, as complete depletion of Q[5] from the beads was observed in the presence of excess salt (section 2.2.1), it is necessary to investigate its consequence on drug release.

As shown in Figures 2.5-2.8, the presence of 0.5mol/L NaCl significantly increased the final percentage of drug released (to 80-100%) for all the formulations of the precursor solutions studied at different pH, compared to their release in water (~50% for ABZ@Q[7] and less than 20% for ABZ@Q[8]). The very high percentage of drug released in the presence of excess salt suggested a substantial electrostatic attraction between the drug complexes and alginate. The higher percentage of ABZ@Q[7] released in water than ABZ@Q[8] suggests that it has a weaker interaction with the hydrogel.

From section 2.2.1, the depletion of Q[5] should be completed within 4 hours in 0.5mol/L NaCl. As a consequence, this seemed to be the maximum duration of bead integrity and drug release in aqueous NaCl, where alginate cannot be protonated to hold the gel. However, the release of

the drug complexes were longer than 4 hours (6-7 hours for ABZ@Q[7] and more than 8 hours for ABZ@Q[8], Figures 2.5-2.8) in aqueous NaCl. Therefore, the depletion of Q[5] was retarded by the presence of the drug complexes and this may support an argument for aggregation of the drug complexes with Q[5] as discussed in section 2.2.4.

Positive correlations of the cumulative release and the release rate to the pH-dependent swelling manifested in the presence of excess salt, to the contrary of the salt-free conditions. There is a noticeable trend of a decreasing percentage of the cumulative release of ABZ@Q[8] in the order of pH1 < pH3 < pH6.3 (Figure 2.5). This order is consistent with the different degrees of swelling under the three pH conditions (Figure 2.2); while the release rates in the three media were similar during the first 30 minutes, release curves of pH3 and pH1 deviated from that of pH6.3 after 30 minutes and the curve of pH1 deviated from that of pH3 after 4 hours. As the Q[5] cross-linker gradually left the beads, a lower pH maintained a denser network to retard the release and entrap ABZ@Q[8]. However, ABZ@Q[7] was insensitive to different pH in the presence of excess salt (Figures 2.7 and 2.8), which implies again its smaller effective size.

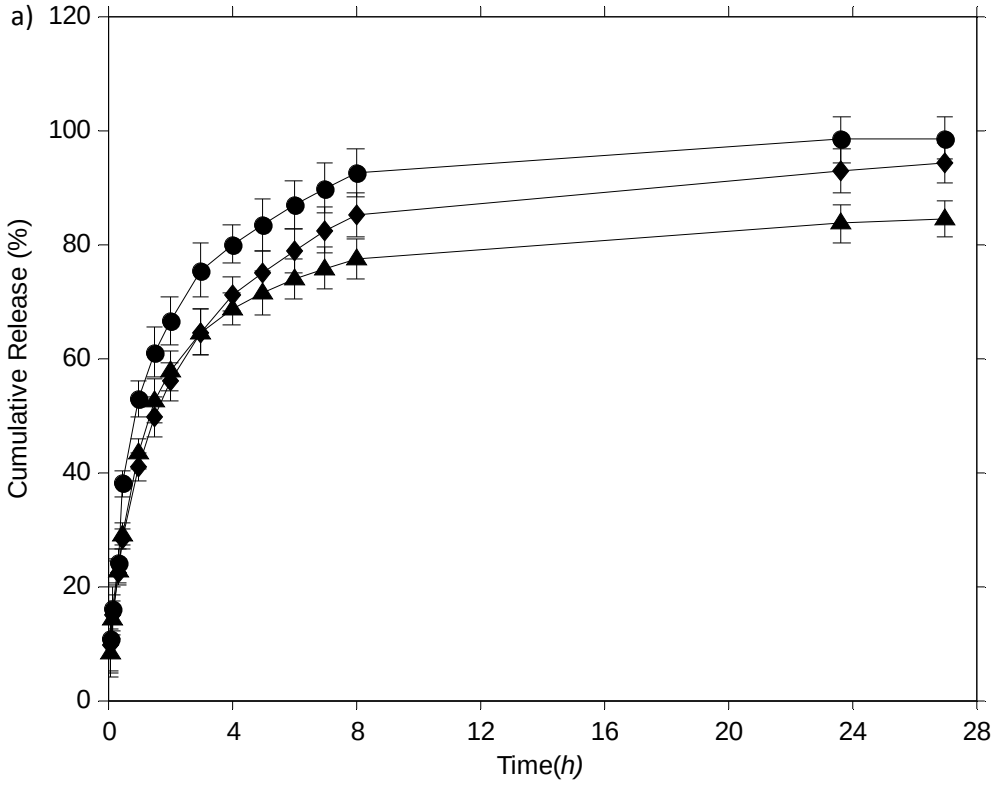


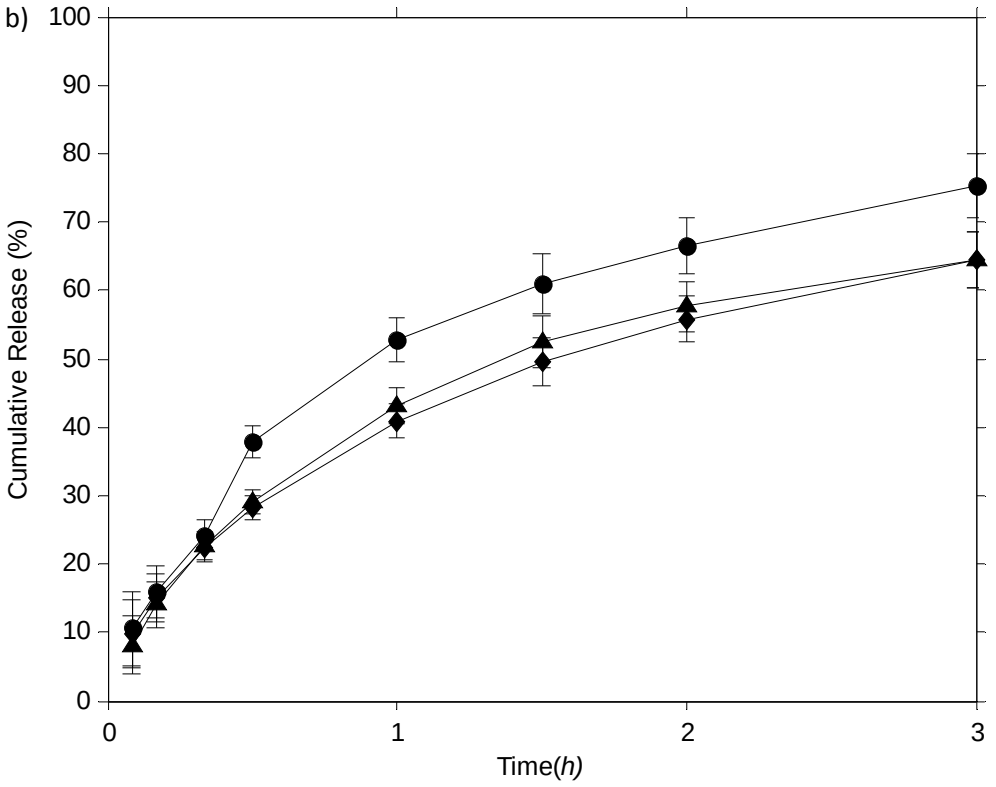


**Figure 2.5 (a) Release of ABZ@Q[8] (8B-high) in release media of aqueous NaCl (●), pH3 NaCl (◆) and pH1 NaCl (▲). (b) Close up look for the first 3 hours.**

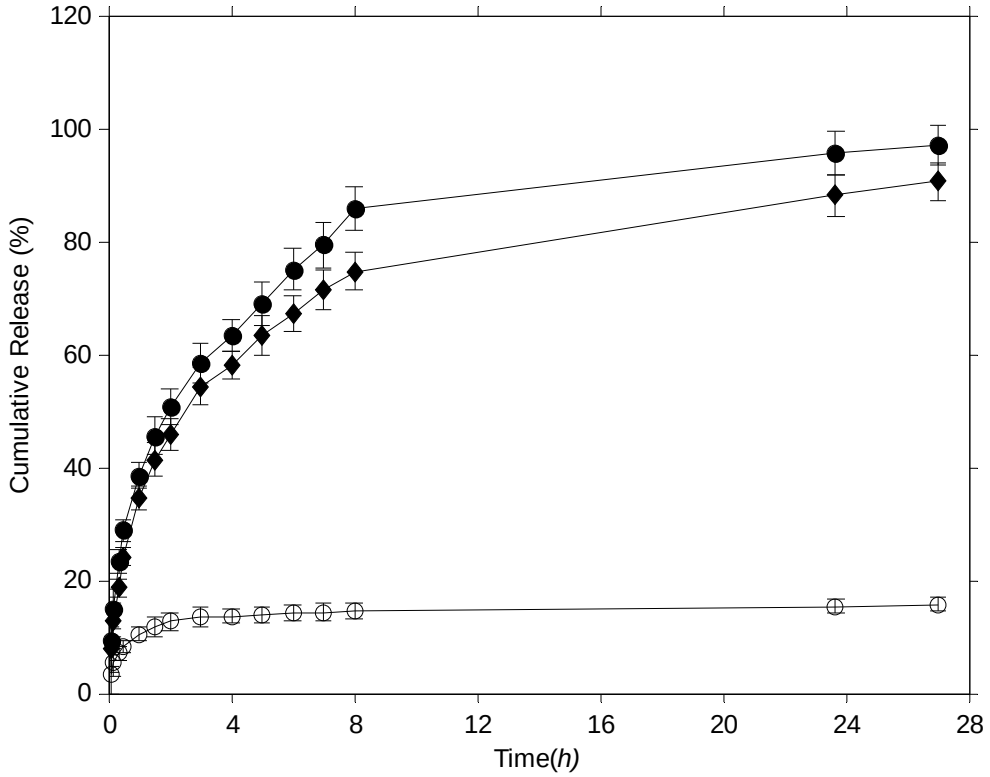


**Figure 2.6 Release of ABZ@Q[8] (8B-low) in release media of water (○), aqueous NaCl (●) and pH3 NaCl (◆).**

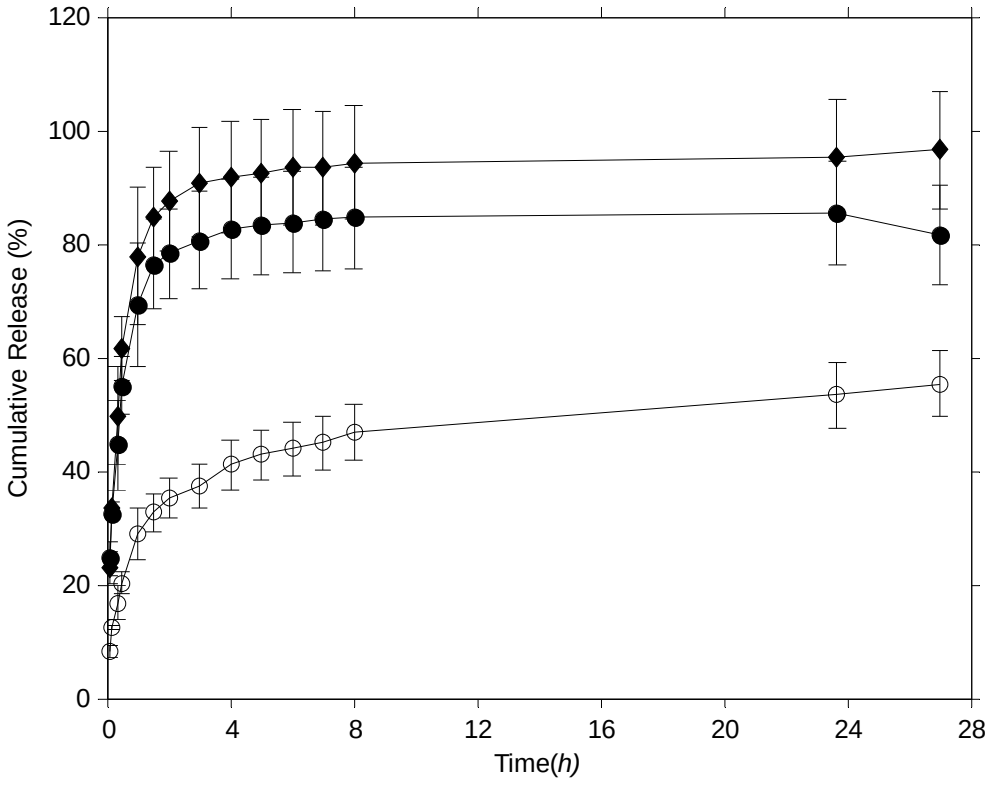


**Figure 2.7 Release of ABZ@Q[7] (7B-low) in release media of water (○), aqueous NaCl (●) and pH3 NaCl (◆).**

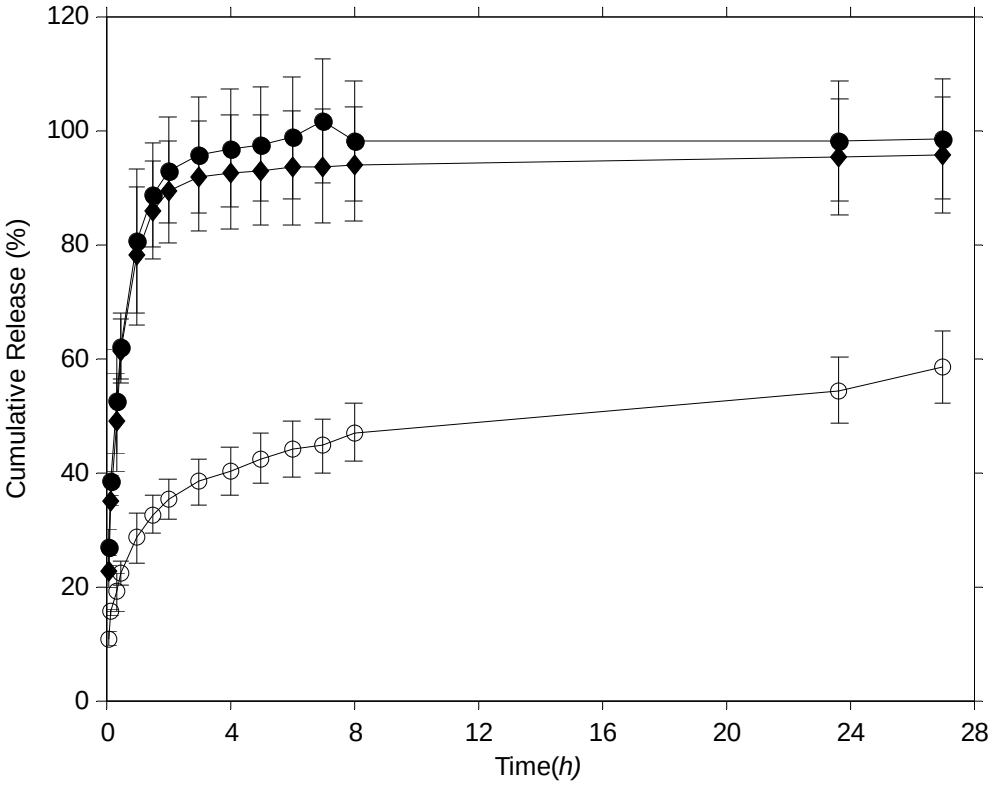


**Figure 2.8 Release of ABZ@Q[7] (7B-high) in release media of water (○), aqueous NaCl (●) and pH3 NaCl (◆).**

### 2.2.3.5 The effect of drug loading amount on drug release

Comparing the release curves presented in Figures 2.4-2.8, it is not surprising that the drug loading amount had no influence on the final percentage of drug released where excess salt was present, as almost all the drug loaded was released. For the salt-free conditions, the final percentage of drug released was not influenced by the drug loading amount, either.

The release rate of ABZ@Q[7] in terms of percentage release was high and almost the same for both high and low loading in the presence of excess salt, with more than 90% of the loaded drug released within the first 4 hours of the release studies (Figures 2.7 and 2.8). However, in 0.5mol/L NaCl, beads of low loading ABZ@Q[8] exhibited lower release rate during 2 to 8 hours of release than those of high loading, and had a more substantial release after 8 hours (Figure 2.9). The gradual release of ABZ@Q[8] resulted in a more porous gel structure and this could be more significant in the case of high loading, which could partially explain the higher release rate observed in Figure 2.9.

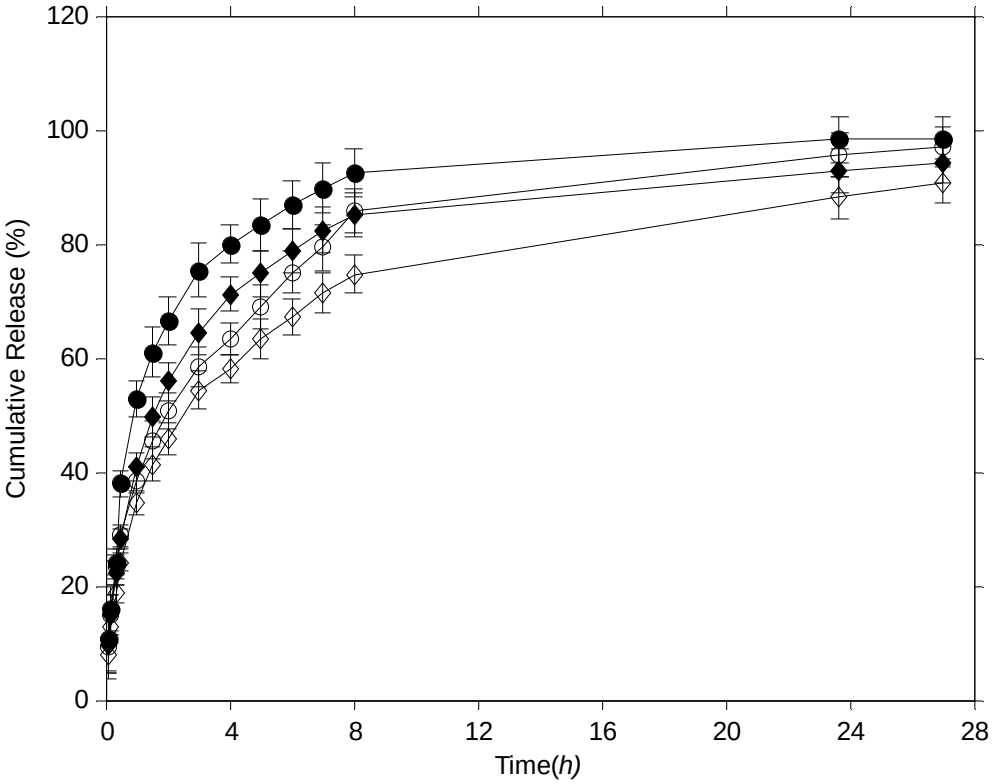


**Figure 2.9 Comparison of ABZ@Q[8] release from beads of high loading (filled symbols ● ◆) and low loading (open symbols ○ ◇) in aqueous NaCl (circle ● ○) and pH3 NaCl (diamond ◆ ◇).**

### 2.2.3.6 Different release behaviour between ABZ@Q[7] and ABZ@Q[8] and drug uptake experiments

There are several differences in the release behaviour of ABZ@Q[7] and ABZ@Q[8] that can be readily drawn from the data of Figures 2.4-2.8. Firstly, the percentage of ABZ@Q[7] released over the period of 28 hours in water was higher than ABZ@Q[8]. Secondly, the release of ABZ@Q[7] was much faster than ABZ@Q[8] provided that excess salt was introduced, where fastest release of the former occurred in 4 hours while the latter up to 8 hours. Lastly, the standard deviation of ABZ@Q[7] release was always larger than that of ABZ@Q[8].

While the difference in standard deviation could be mainly attributed to the lower ABZ:Q[*n*] ratio of ABZ@Q[7] than that of ABZ@Q[8] (Table 2.1), reasons for the differences in the percentage of drug complex released and the release rate are not obvious, as similar behaviour could be expected for the two homologues.

In the above experimental results and discussion of this section, there have been implications that ABZ@Q[7] has a lower affinity to the hydrogel and smaller effective size than ABZ@Q[8]. In order to sustain such differences of the drug complexes and to get a further insight of how

they interact with the beads, uptake of the drug complexes by empty alginate beads were studied. The potential effects of different drug loading methods on the drug release profile may also be revealed.

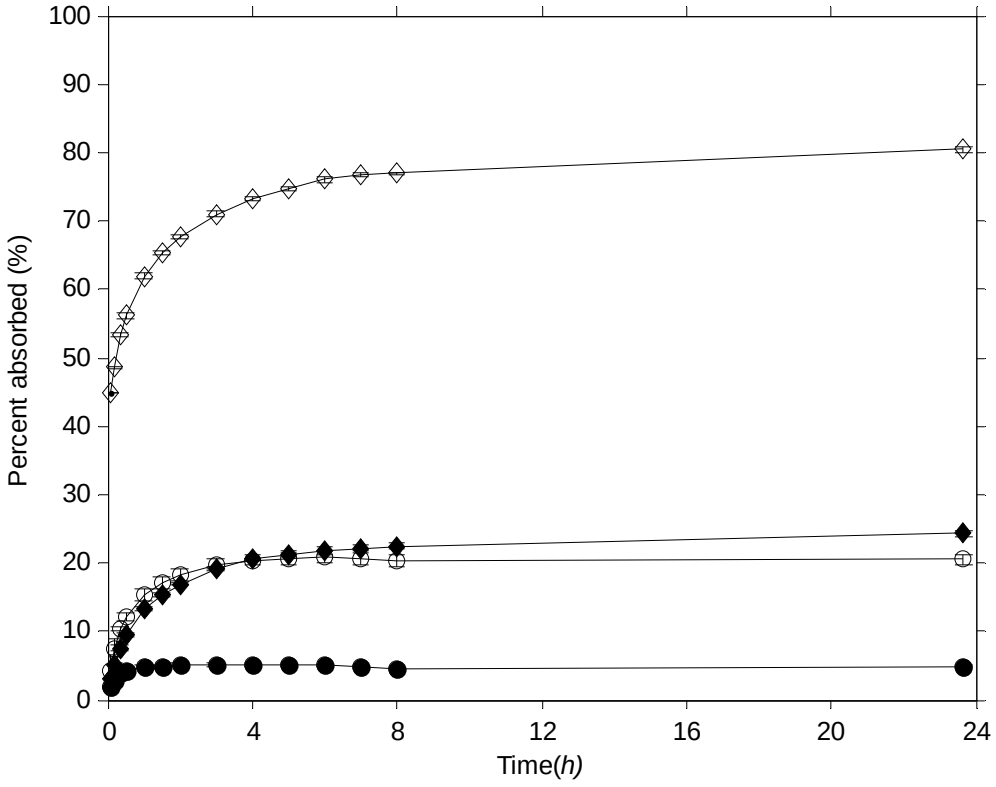


**Figure 2.10 Uptake of ABZ@Q[7] (circle ● ○) and ABZ@Q[8] (diamond ◆ ◇) by empty alginate beads in near-neutral solutions (open symbols ○ ◇) and pH3 0.5mol/L NaCl solutions (filled symbols ● ◆). The initial UV absorbance of the drug complex solutions was maintained at around 1, which corresponds to an ABZ concentration of ~0.1mmol/L.**

As shown in Figure 2.10, there is a very large difference in the uptake of ABZ@Q[7] and ABZ@Q[8] by empty alginate beads. At equilibrium in salt-free solutions, 80% of the ABZ@Q[8] available was absorbed while it was only 20% for ABZ@Q[7]. The presence of excess salt, as expected, impeded the uptake of the drug complexes greatly. However, there was still more than 25% of the ABZ@Q[8] absorbed while the absorption of ABZ@Q[7] was only ~5%.

The radius of the beads was ~1.5mm and the volume of the 3 beads was less than 1.5% of the 3mL solution. The decreased concentrations of the drug complexes in the solutions were therefore not the result of dilution. In all the 4 cases, a higher concentration of the drug complex was maintained in the beads. The much higher percentage of ABZ@Q[8] uptake reflects its higher affinity to the hydrogel than ABZ@Q[7]. Moreover, substantial uptake of ABZ@Q[*n*] even at a salt concentration of 5000 times, especially in the case of ABZ@Q[8],

suggests that electrostatic attraction cannot be the sole reason for the observed affinity of ABZ@Q[*n*] to the alginate hydrogel.

The drug release from beads loaded by this soaking method is shown in Figure 2.11. Release of ABZ@Q[7] was as high as 50%, in contrast to ~5% for ABZ@Q[8]. The amount of ABZ@Q[7] loaded by the soaking method, normalized against the hydrogel weights, was approximately 2 times of the low loading beads. For ABZ@Q[8], this value was comparable to the high loading beads. Therefore, different drug loading methods did not have significant effects on the cumulative release of ABZ@Q[7] (all ~50%), but the release of ABZ@Q[8] from the beads loaded by the soaking method was impeded to a greater extent than from those loaded by mixing ABZ@Q[8] in the precursor solutions (more than 10% as oppose to ~5% here).

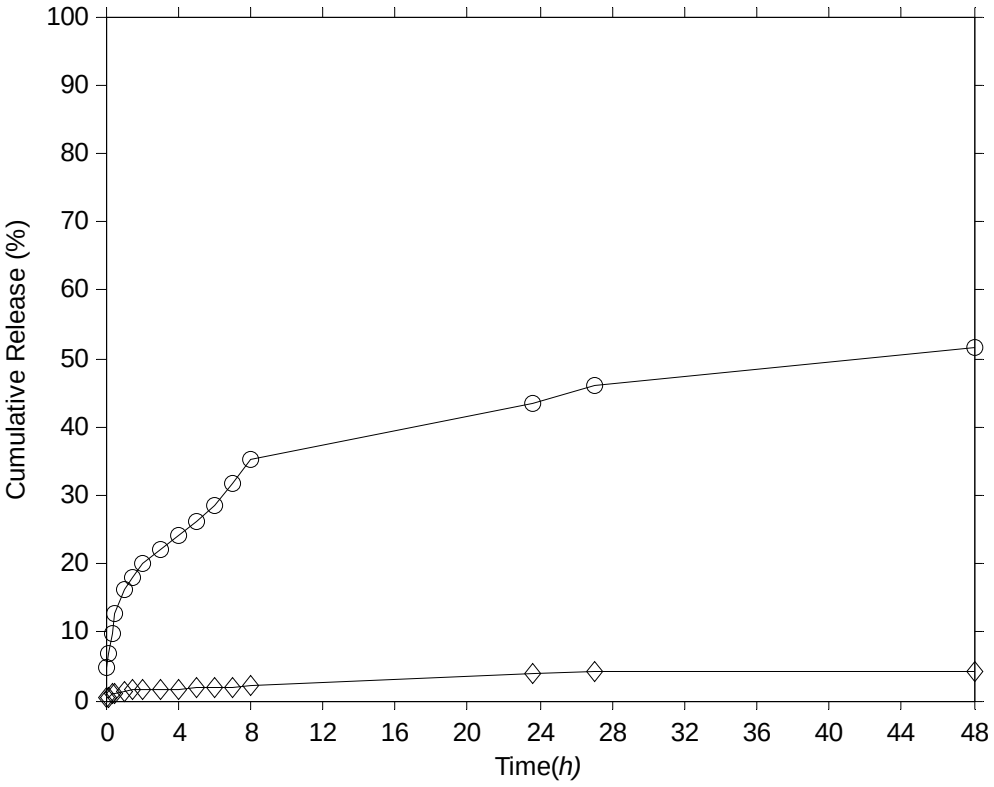


**Figure 2.11 Release of ABZ@Q[7] (○) and ABZ@Q[8] (◇) in water from alginate beads loaded by the soaking method.**

### 2.2.4 The proposed structure of the drug delivery system and the release mechanism

From the results presented in section 2.2.3, it is seen that there was strong binding of the drug complexes to the alginate beads, with ABZ@Q[8] exhibiting a greater degree of affinity than ABZ@Q[7]. Upon the introduction of excess sodium chloride or the protonation of alginate,

the bonded drug complexes are freed and this enables substantial release. Therefore, such binding appeared to be primarily due to electrostatic attraction. However, it was also facilitated by other interactions (section 2.2.3.6), as will be discussed.

There have been many studies on the binding of surfactants to polyelectrolytes (of which alginate is an example) in aqueous media, which suggests that it is a complicated process influenced by many factors such as the ionic strength of the media, the conformation of the polyelectrolyte, cross-linking of the polyelectrolyte, and the length of the lipophilic section of the amphiphiles [103-108]. The results of such studies were typically presented as binding isotherms as shown in Figure 2.12, where the degree of binding (*β*), defined as the molar ratio of bound surfactant to the total ionic group in the polyelectrolyte, was plotted against the free surfactant concentration ($m_D^f$ or its logarithm). The sigmoidal curve is characteristic for a so-called "cooperative binding" mechanism, where the binding is not only derived from electrostatic interactions but is also facilitated by hydrophobic interactions, in the case of some surfactants, between the bound ions [107]. In fact, two parameters, *K* and *u*, were introduced to describe the cooperative binding curve. *K* is the binding constant of the surfactant to an isolated binding site, driven solely by electrostatic attraction. It reflects the onset of the curve. *u* is the cooperativity parameter describing the degree of hydrophobic interaction between adjacently bound ions and is reflected by the steepness of the curve. Generally, the binding isotherms will be pushed to the right hand side with increased concentration of inorganic salt, as shown by curves a-f in Figure 2.12.

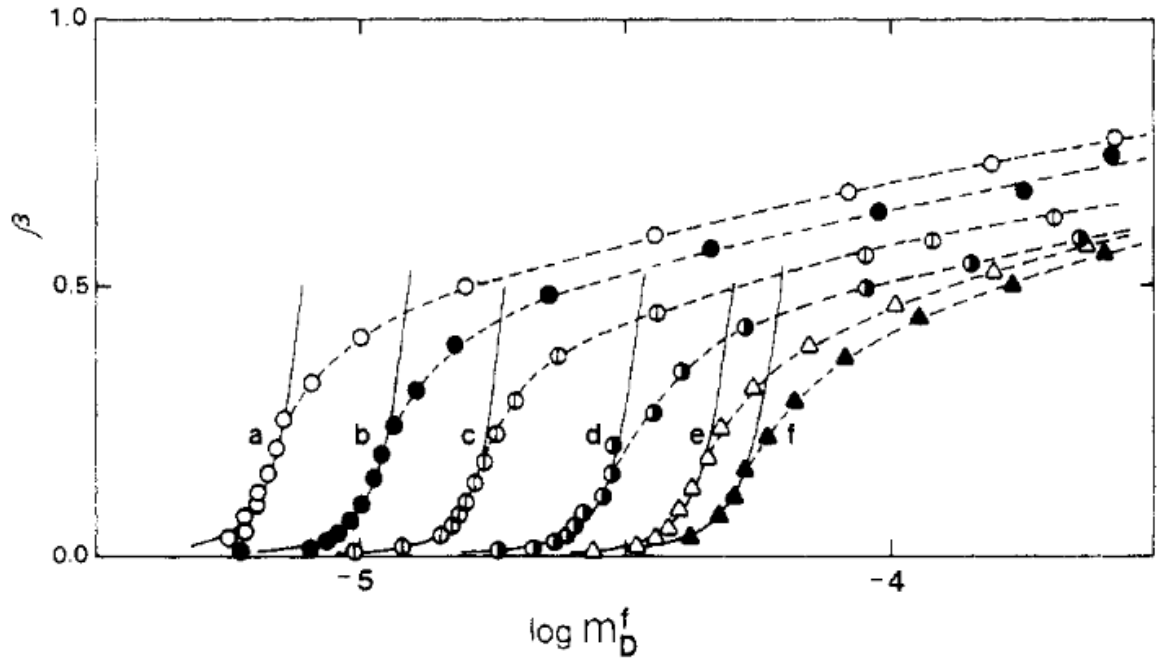


**Figure 2.12 Binding isotherms of surfactant by polyelectrolyte. Curves a-f reflect the effect of increased NaCl concentration. Figure taken from [107].**

As discussed in section 2.2.3.4, depletion of Q[5] from the beads was retarded in the presence of the drug complexes. It is possible that the drug complexes formed aggregates with Q[5], through intermolecular interactions such as ion-dipole interactions and hydrogen bonding. As such, the drug complexes would have sigmoidal binding curves similar to those of surfactant binding. With excess salt, the binding curves of the drug complexes were pushed to the right due to the competitive binding of the sodium to the carboxylate groups of alginate. Hence most of the aggregates could be released and little of them could remain bonded. The different absorption and release behaviours of ABZ@Q[7] and ABZ@Q[8] could be then explained by their different "cooperativity" with themselves and Q[5]. With stronger interactions with itself and Q[5], ABZ@Q[8] could maintain larger aggregates than Q[7], which sustained a more drastic concentration difference between the hydrogel beads and the surrounding media, hence the observed higher absorption and lower release in water.

The discussion above is based on Q[*n*] having a similar cooperative mechanism to that of surfactants in addition to their interaction with the oppositely charged polyelectrolyte, but there is no direct evidence confirming the formation of such aggregates. Thus, this hypothesis needs to be confirmed by further investigation. However, it is worth noting that interactions between the hydrophobic surfaces of Q[*n*] have been demonstrated by the Q[5]@Q[10] complex [109]. Additionally, ordered structure of Q[*n*] in the solid state can serve as tenuous

evidence. Three Q[5] molecules coordinated to potassium ions form planar trigonal branches when templated on a molecule of *p*-hydroxybenzoic acid which locates centrally over the junction [110]. Such trigonal branches can form hexagonal rings which stack layer by layer in the solid state.

### 2.2.5 Release of drug complexes in physiological saline

Based on the above observations and discussion, it could be anticipated that the performance of the combined drug delivery system of alginate and Q[*n*] for albendazole would be affected by the moderate number of ions present under physiological conditions. The results for the release of the two ABZ@Q[*n*] drug complexes in physiological saline are shown in Figure 2.13. The percentage of both drug complexes released were higher than in water, but the time period for substantial release was more prolonged than in concentrated NaCl. For ABZ@Q[8], the fastest release period occurred over a day followed by a slower release over the next 5 days. For ABZ@Q[7], the fastest release time period doubled to 8 hours, compared to that in 0.5M NaCl.

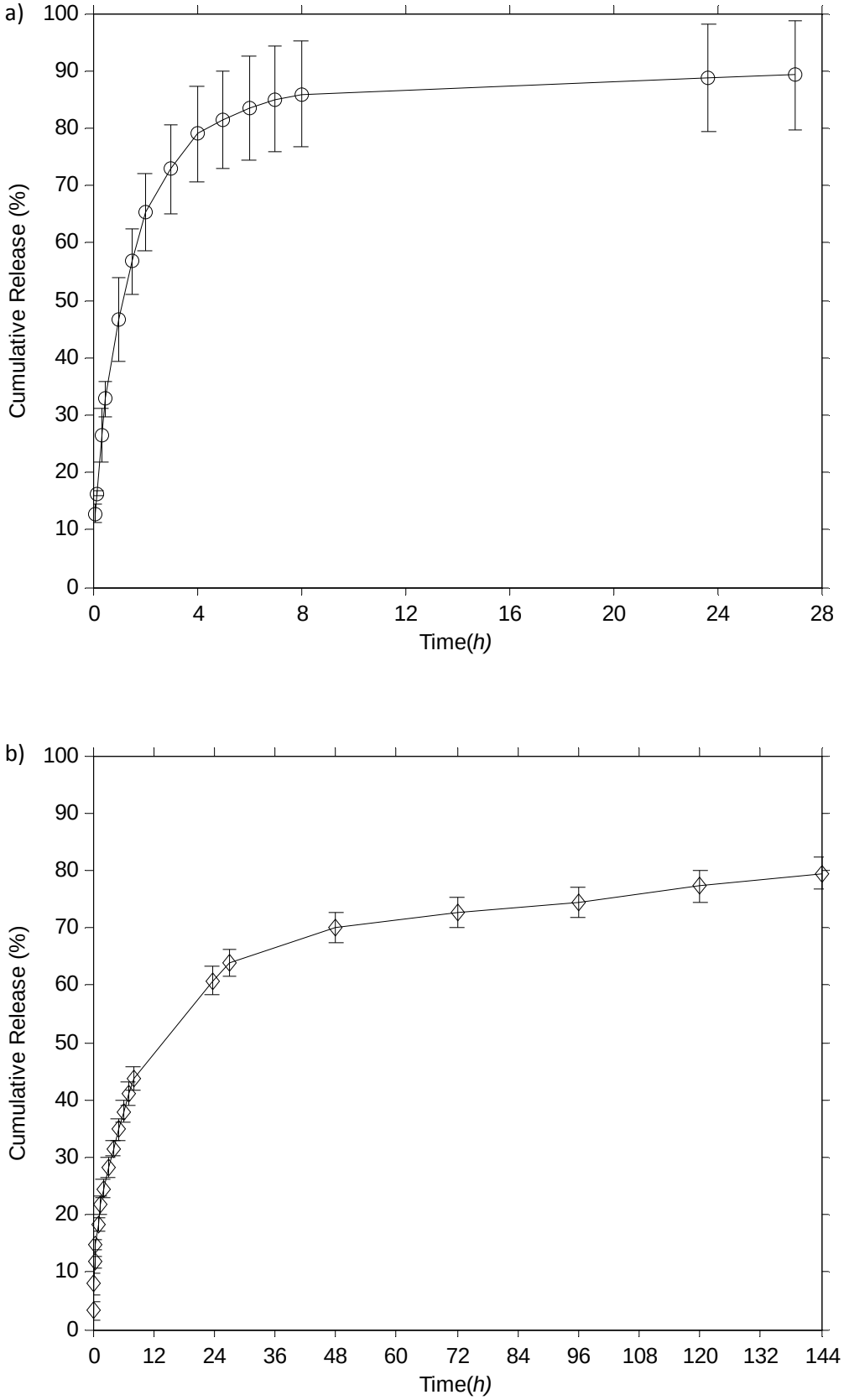


**Figure 2.13 Release of ABZ@Q[7] (7B-high) (a) and ABZ@Q[8] (8B-high) (b) in physiological saline.**

## 2.3 Conclusion

In the experimental part of this work, the sparingly soluble drug ABZ was successfully loaded into an alginate hydrogel through encapsulation in Q[7] or Q[8]. The drug loading content and efficiency were found to increase significantly, compared to the case where ABZ was supplied as a suspension.

The percentage of drug released was found to be sensitive to the concentration of NaCl and pH. In the presence of excess salt, almost all of the loaded drug could be released. Under these conditions, the release rate was mainly dependent on the encapsulating Q[*n*] used. Different uptake by the empty beads reflected the different affinity of ABZ@Q[*n*] to the hydrogel. Considering the experimental results together, it is tentatively suggested that ABZ@Q[*n*] formed aggregates of different sizes with Q[5], thus had their effective size increased and their release retarded to different degrees.

In physiological saline where drug delivery systems are applied, ABZ@Q[8] achieved prolonged release over several days and ABZ@Q[7] exhibited faster release and can provide higher concentrations. Some of the mechanisms identified here will be evaluated via simple modelling in the following chapter.

# Chapter 3 Mathematical modelling

## 3.1 Introduction

The benefits of an accurate mathematical description of mass transport in controlled drug delivery systems can be two-fold: giving clear insight into the release mechanism of a particular system and predicting the design parameters to achieve a required release profile [111, 112]. However, different mass transport mechanisms entangle to make such a precise description difficult. Although simple and sophisticated mathematical models have been proposed, they were built on one or a few rate-limiting steps. For systems where diffusion is the predominant step, the effective diffusion coefficient can be obtained by fitting experimental data to equations derived from Fick's laws of diffusion for different geometries. The diffusion coefficients can also be predicted by numerous models, provided that necessary properties of the release system are well characterized, as discussed in the first chapter.

## 3.2 Identifying the controlling step of release

Identifying the rate-limiting step is essential for finding an appropriate model to describe drug release from the delivery system in this study. A power law was introduced to identify the controlling drug release mechanism and is known as the "Peppas equation" [111], as given by equation (3.1).

$$\frac{M_t}{M_\infty} = kt^n \qquad (3.1)$$

Here, $M_t / M_\infty$ is the cumulative drug release at time *t* normalized by the total drug released and *k* is a characteristic constant incorporating the parameters that describe the system. The diffusion exponent, *n*, is indicative of the release mechanism, when the first 60% of $M_t / M_\infty$ from experimental data is fitted to the equation [111]. The correlations between the fitted *n* and the drug release mechanism for different geometries are tabulated in Table 3.1.

**Table 3.1 Diffusion exponent *n* and drug release mechanism for different geometries. Values taken from [111].**

| Thin film | Cylinder | Sphere | Drug release mechanism |
|---|---|---|---|
| 0.5 | 0.45 | 0.43 | Fickian diffusion |
| 0.5<*n*<1.0 | 0.45<*n*<0.89 | 0.43<*n*<0.85 | Anomalous transport |
| 1.0 | 0.89 | 0.85 | Case-II transport |

Cumulative release was normalized by total drug released, as determined from the plateau value towards the end of the drug release studies, and the first 60% was fitted to equation (3.1) in the least-squares sense using the trust-region reflective algorithm incorporated in MATLAB. Values thus obtained and the identified release mechanisms for the drug release under different conditions are shown in Table 3.2.

**Table 3.2 Fitted values of the parameters for drug release under different conditions.**

| Release condition | *n* | *k* | $R^2$ | Drug release mechanism | $D_{eff}$ ($cm^2/s$) |
|---|---|---|---|---|---|
| 7B-low, water | 0.4329 | 0.0833 | 0.9908 | Diffusion | $1.4612\times10^{-7}$ |
| 7B-low, aqueous NaCl | 0.4574 | 0.1346 | 0.9978 | Anomalous | $6.8108\times10^{-7}$ |
| 7B-low, pH3 NaCl | 0.5492 | 0.1001 | 0.9998 | Anomalous | $6.5512\times10^{-7}$ |
| 7B-high, water | 0.3497 | 0.1233 | 0.9964 | Diffusion | $1.6236\times10^{-7}$ |
| 7B-high, aqueous NaCl | 0.4593 | 0.1332 | 0.9983 | Anomalous | $6.9878\times10^{-7}$ |
| 7B-high, pH3 NaCl | 0.5367 | 0.1031 | 0.9975 | Anomalous | $6.5921\times10^{-7}$ |
| 7B-high, physiological saline | 0.5265 | 0.06 | 0.9975 | Anomalous | $2.2830\times10^{-7}$ |
| 8B-low, water | 0.4068 | 0.1291 | 0.9851 | Diffusion | $3.5707\times10^{-7}$ |
| 8B-low, aqueous NaCl | 0.4449 | 0.0617 | 0.9901 | Anomalous | $1.0569\times10^{-7}$ |
| 8B-low, pH3 NaCl | 0.4369 | 0.054 | 0.9882 | Anomalous | $6.8797\times10^{-8}$ |
| 8B-high, water | 0.4184 | 0.1145 | 0.9965 | Diffusion | $2.0583\times10^{-7}$ |
| 8B-high, aqueous NaCl | 0.5801 | 0.0474 | 0.9792 | Anomalous | $1.8814\times10^{-7}$ |
| 8B-high, pH3 water | 0.4373 | 0.0774 | 0.9929 | Anomalous | $1.4739\times10^{-7}$ |
| 8B-high, pH3 NaCl | 0.5227 | 0.0496 | 0.9973 | Anomalous | $1.3877\times10^{-7}$ |
| 8B-high, pH1 water | 0.5955 | 0.0469 | 0.9983 | Anomalous | $2.4315\times10^{-7}$ |
| 8B-high, pH1 NaCl | 0.589 | 0.0448 | 0.9955 | Anomalous | $1.8225\times10^{-7}$ |
| 8B-high, physiological saline | 0.427 | 0.039 | 0.9935 | Diffusion | $2.8727\times10^{-8}$ |

All the fitted curves agreed well with the experimental data, as indicated by the values of $R^2$. From the fitted values of *n*, drug release in water seemed to be controlled by pure diffusion, while excess salt and/or in acidic pH gave rise to anomalous release (both diffusion and swelling controlled release). It should be noted however, that experimental uncertainty plays a role here. Given the values of the fitted *n*, it is likely that most of these systems could be modelled by a diffusion mechanism (as will be demonstrated in the following section).

Purely swelling-controlled drug release (Case-II transport) is typically observed in tablets formed by compressing a powdered mixture of hydrogel, drug and other excipients, where drug is restrained from release until the influx of the release medium, which swells the tablet, dissolves the drug and enables drug release, and is much slower than the subsequent diffusion of the drug [113]. In our case, the swelling-controlled component in drug release is due to the increased porosity of the hydrogel, also due to the cross-linking Q[5] being pushed out, as well as a decrease in the internal concentration of the drug as the bead swells uniformly.

It is expected that the value of *k* correlates inversely with the molecular weight [113] and diffusion coefficient [111]. The fitted values of *k* for ABZ@Q[7] are approximately two times that of ABZ@Q[8] in the same release medium, except for those in water. The fitted *k* values are consistent with a faster diffusion of the Q[7] complex, which correlates with a lower binding affinity with the gel and presumably a smaller effective size.

The fitted *k* values for ABZ@Q[8] in water are unreasonably large. This is because the initial burst release makes up a very large proportion of the very small amount of drug released, exaggerating the release rate. Therefore, the fitted values of *k* under these conditions are not reliable for comparison. This is further discussed in the following section.

## 3.3 Fitting to a diffusion equation

Diffusion controlled drug release can be modelled by equations obtained by solving the partial differential equation of Fick's second law of diffusion (equation (3.2), assuming a constant diffusion coefficient $D_{\text{eff}}$), using different boundary conditions according to the different setups of the delivery system. The drug delivery system in this study is assumed to be a monolithic device, wherein the drug is homogeneously distributed throughout the hydrogel matrix within its solubility (Table 2.5)[112]. The corresponding boundary conditions are given in equation (3.3) [114]. The analytical solution has been derived by Crank, as given by equation (3.4).

$$\frac{\partial C}{\partial t} = -D_{eff}\frac{\partial^2 C}{\partial r^2} \qquad (3.2)$$

$$C(r < a, t = 0) = C_0$$
$$C(r = a, t = 0) = 0 \qquad (3.3)$$
$$C(r < a, t = \infty) = 0$$

$$\frac{M_t}{M_\infty} = 1 - \frac{6}{\pi^2} \sum_{n=1}^{\infty} \frac{\exp\left(-Dn^2\pi^2 t / R^2\right)}{n^2} \qquad (3.4)$$

The following assumptions are made when applying the equation to release data.

- Diffusion is the rate-limiting step in drug release.
- The diffusion coefficient of the drug is constant.
- Perfect sink conditions are provided in the release medium over the timeframe of release study.
- Swelling or shrinking of the device is negligible or equilibrium is reached rapidly.
- Erosion of the device is negligible.
- Unstirred boundary layer of the release medium on the surface of the device is thin so that mass transfer resistance is negligible.

Most of the assumptions are readily satisfied. However, significant swelling of the beads was observed on the same time scale of drug release, as described in section 2.2.2 and there is a swelling controlled component in most cases. Rasmussen et al. developed a numerical model for protein release from swelling calcium alginate beads, and concluded that the release of smaller proteins such as insulin hexamer (39kD) can be satisfactorily modelled by a non-swelling diffusion model [115]. The component that accounts for the effects of swelling had to be included only for larger proteins such as amyloglucosidase (97kD) to achieve a good agreement between the theoretical curve and the experimental data [115]. The drug complexes in our study, even in the form of aggregates, are presumably smaller than proteins. The swelling controlled component effectively raised the effective diffusion coefficient. In fact, if good agreement between the fitted curve and the experimental data can be achieved when a non-swelling diffusion equation is applied, the effects of hydrogel swelling and the swelling controlled component are accounted for in the fitted effective diffusion coefficient [115]. Therefore, the effective diffusion coefficients ($D_{eff}$) obtain by fitting equation (3.4) to drug release data, as listed in Table 3.2, are at least valid for comparisons within this study, although they may not be accurate values for the intrinsic diffusion coefficients of the drug complexes in the alginate network.

The experimental data used and the curve fitting method were the same as in section 3.2, but the full range of $M_t / M_\infty$ (from 0 to 1) was used, rather than from 0 to 0.6. The infinite series of exponential function in equation (3.4) was restricted to 50 terms to give a balance between accuracy and efficiency. The difference between increasing the number of terms and restricting it to 50, even at the smallest time interval, was negligible in terms of experimental error.

As can be seen from Figures 3.1-3.5, with a fitted effective diffusion coefficient, curves given by the diffusion equation (dash-dot line) agreed very well with experimental points (symbols) in all the release media (Figure 3.2-3.5) except water (Figure 3.1). While the theoretical curves are accurate for the first ~70% of drug released in water, the experimental points deviated from the theoretical curves in the later stage of release. As discussed in section 3.2, this is because an initial burst release of drug contributed to a very large proportion of the total drug released. Drug release in the later stage is overestimated by the fitted $D_{\text{eff}}$ as it is likely that retardation due to drug bound to the alginate asserts itself. This is supported by the fact that the deviation for ABZ@Q[8] is greater than ABZ@Q[7], as could be expected because ABZ@Q[8] appears to associate more strongly with the gel than ABZ@Q[7].

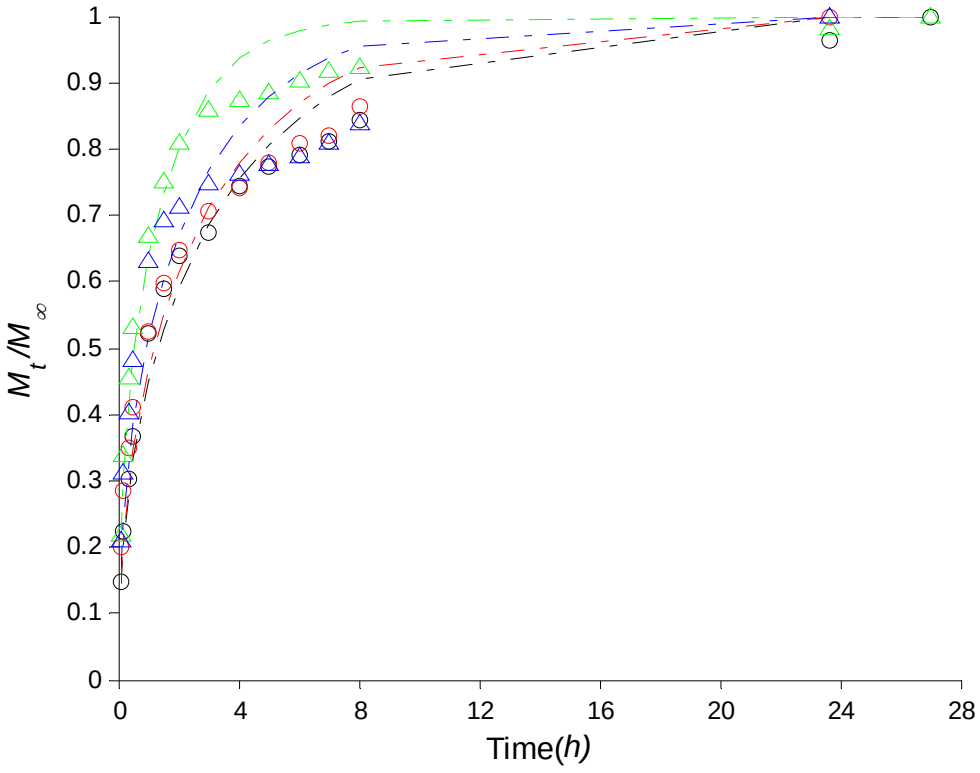


**Figure 3.1 Release of 7B-low (black), 7B-high (red), 8B-low (green), and 8B-high (blue) in water fitted to equation (3.4).**

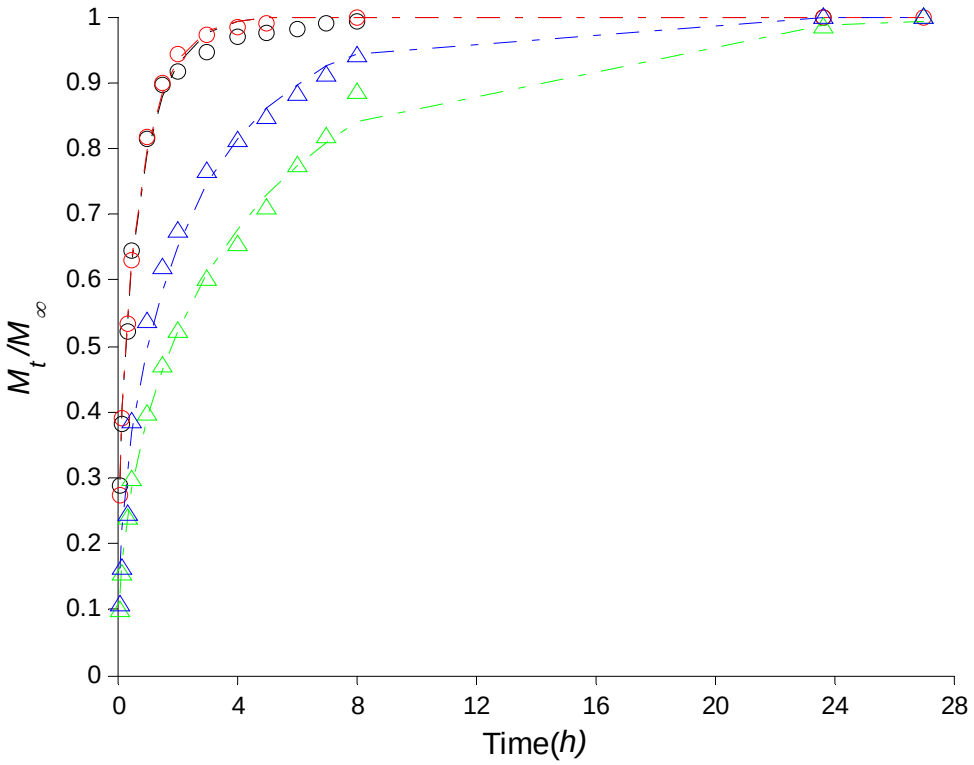


**Figure 3.2 Release of 7B-low (black), 7B-high (red), 8B-low (green), and 8B-high (blue) in aqueous NaCl fitted to equation (3.4).**

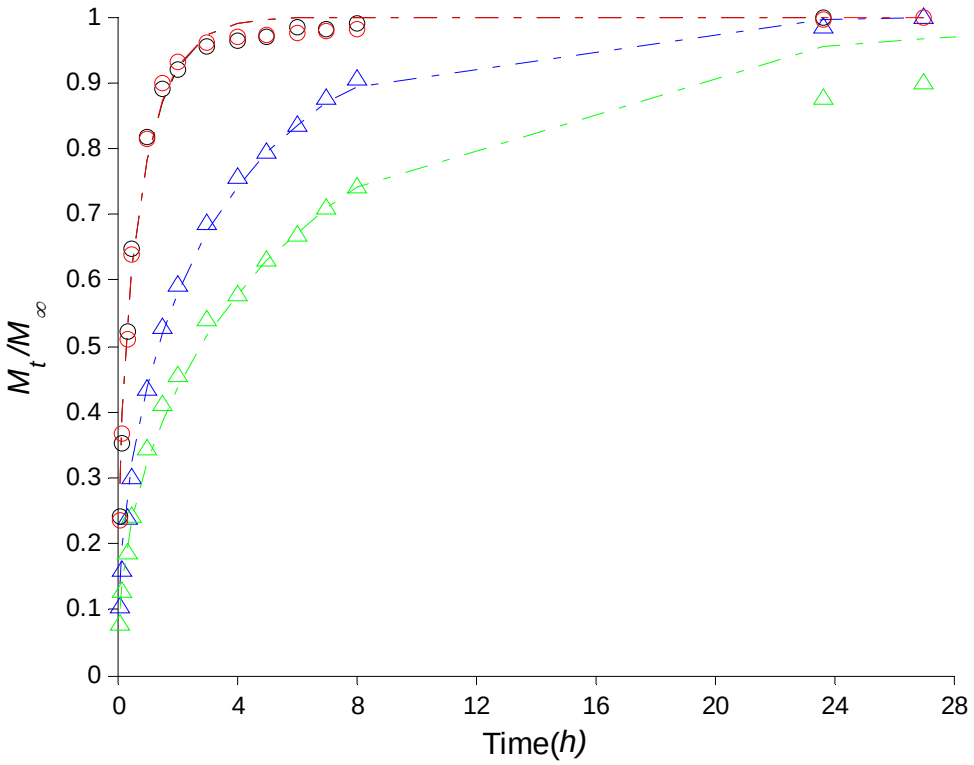


**Figure 3.3 Release of 7B-low (black), 7B-high (red), 8B-low (green), and 8B-high (blue) in pH3 NaCl fitted to equation (3.4).**

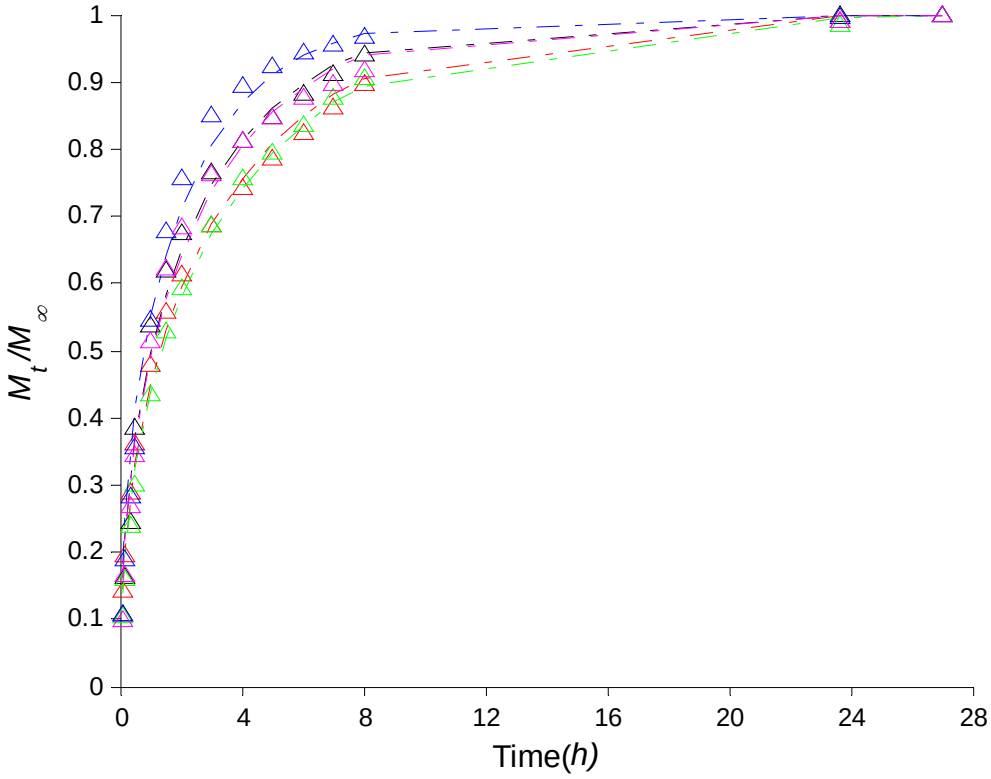


**Figure 3.4 Release of 8B-high in aqueous NaCl (black), pH3 water (red), pH3 NaCl (green), pH1 water (blue), and pH1 NaCl (magenta) fitted to equation (3.4).**

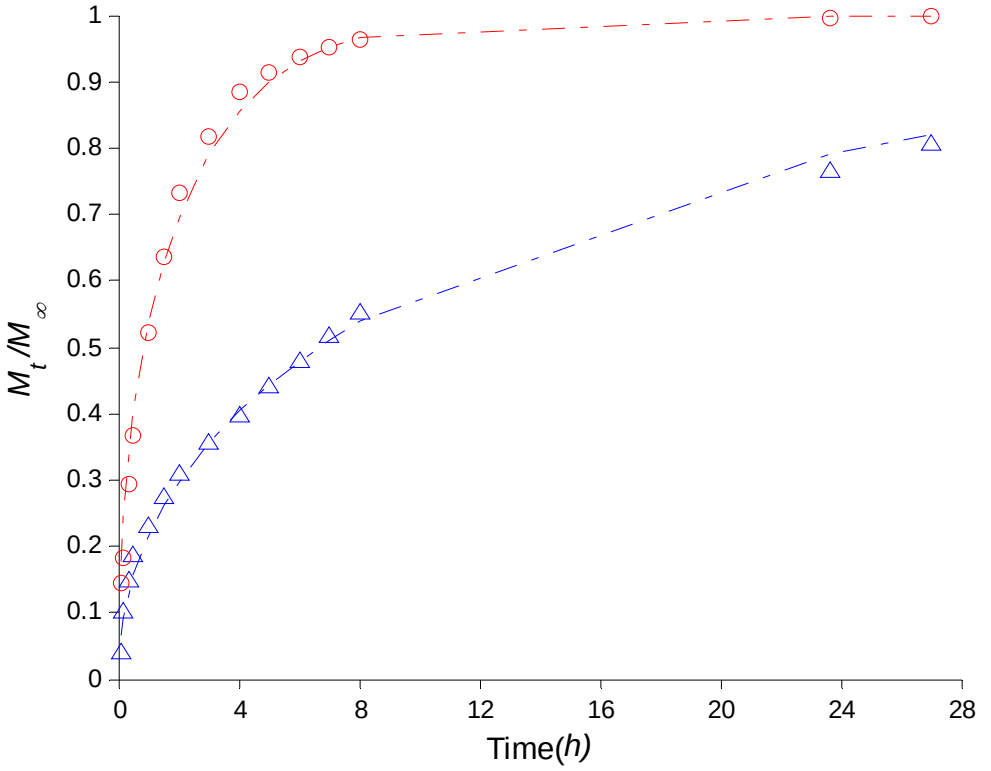


**Figure 3.5 Release of 7B-high (red) and 8B-high (blue) in physiological saline fitted to equation (3.4).**

Comparing the fitted $D_{eff}$ in all the other release media, it is always much larger for ABZ@Q[7] than ABZ@Q[8] in the same release medium. Again, this suggests that the gel binding of ABZ@Q[8] is more pronounced than for ABZ@Q[7]. The effect of high or low loading of ABZ@Q[7] on the fitted $D_{eff}$ is negligible, while low loading of ABZ@Q[8] has a smaller $D_{eff}$ than high loading. This could be due to the mutual screening of ABZ@Q[8]/gel association, an effect that is more significant in high loading.

Apart from the intrinsic properties of the drug complexes and the drug loaded alginate beads, the ionic strength of the release medium and the ion species present also significantly shifted the values of the fitted $D_{eff}$. This is expected from the above discussion. As evidenced by the different values of the fitted $D_{eff}$ in aqueous NaCl and physiological saline, a more concentrated solution of NaCl increased the $D_{eff}$ by more than 3 times, suggesting significant competitive binding of the salt against the drug complexes. The $D_{eff}$ of ABZ@Q[8] in pH1 water is comparable to that in 0.5mol/L NaCl solution. Considering the much lower concentration of $H^+$ than $Na^+$, different ions may have different efficiencies in the competitive binding, providing another opportunity to manipulate the effective diffusion coefficients of the drug complexes. Finally, the $D_{eff}$ in pH3 NaCl is always smaller than its counterparts in aqueous NaCl. The difference, albeit very small, could be the result of a less porous network, which is maintained by a more acidic pH after the Q[5] cross-linker was pushed out together with the drug complexes.

# Chapter 4 Conclusion

With the growing interest in the application of hydrogels as controlled drug delivery systems and the fact that a majority of the new drugs are hydrophobic, there is a pressing demand in alleviating the problems that lie in their inherent incompatibility. In this study, instead of methods such as drug entrapment in liposomes and grafting hydrophobic sections in the network, a macrocyclic host molecule, cucurbit[*n*]uril, is used to mediate the incompatibility between albendazole (ABZ), a sparingly soluble drug, and alginate, through the host-guest encapsulation process. In addition, a smaller homologue in the cucurbit[*n*]uril family, Q[5], with the sodium ions bonded at both of its portals, served as a ionic cross-linker in the alginate beads prepared.

The alginate hydrogel beads fabricated in this study were robust and exhibited the same pH responsive swelling as calcium alginate hydrogels. However, although contributed substantially to the gelation of the beads, Q[5] appeared to be a relative weak ionic cross-linker, as dissolving sodium alginate in saturated Q[5] solution only resulted in a very viscous solution but not a gel. In addition, Q[5] appeared prone to ion exchange, being completely depleted from the beads in concentrated NaCl solution. It has been reported that Q[*n*] of different sizes and their different derivatives have different binding constants to different cations [89-91, 116, 117]. An appropriate combination of the macrocyclic molecule and the cation may therefore result in ionic cross-linkers of different effectiveness, thus controlling the disintegration of the hydrogel under physiological conditions.

The solubility of ABZ was enhanced greatly through the encapsulation in Q[7] and Q[8] and the complexes were loaded into the alginate beads with relatively high efficiency. Release studies were conducted using drug loaded beads of different formulation in different release media to investigate factors controlling drug release. Uptake of the drug complexes by empty alginate beads were also studied to further reveal the different affinity of the drug complexes to the hydrogel. The experimental data were analysed by established mathematical models to identify the drug release mechanism by also comparing the effects of pH and the concentration of NaCl. Collating the experimental observations, with the aid of mathematical models, the following conclusions can be drawn.

The percentage of the loaded drug that can be released varied according to the different homologues and the amounts of the drug complexes loaded. However, the most significant factor was the nature of the release media, which includes pH and the concentration of NaCl. This general description is also valid for the drug release rate. While the release of the drug complexes were purely or mainly controlled by diffusion, substantial release was enabled only in the presence of sodium or hydrogen ions that competed with the aggregates formed by the drug complexes and Q[5] in the binding to the alginate chains. This competitive binding introduced a swelling controlled component to the drug release mechanism. Therefore, the effective diffusion coefficient is correlated to pH and the concentration of NaCl. The effect of the swelling degree on drug release was perceptible only in the cases where this competitive binding was observed, it was otherwise masked by the ineffective release of the drug complexes.

A very interesting result of this study is the drastic difference between ABZ@Q[7] and ABZ@Q[8], which was not expected for these homologues. ABZ@Q[8] had higher loading efficiency, slower release and stronger absorption into empty alginate beads than ABZ@Q[7]. These observed differences are all attributable to the difference in their “cooperativity” with themselves and Q[5] and their interaction with the gel. Presumably, ABZ@Q[8] can form more robust and larger aggregates on Q[5] and this is supported by the fitted parameters of the mathematical models. This offers a novel method of controlling the effective size of the diffusing agent and hence the release profile.

In physiological saline, release of ABZ over several days was achieved by ABZ@Q[8] loaded alginate beads and ABZ@Q[7] loaded beads provided faster release and higher ABZ concentration. Based on the results of this study, it is anticipated that the strength of the ionically cross-linked hydrogel, its rate of disintegration, and the effective size of the diffusing drug can be manipulated through a careful selection of cucurbit[*n*]uril and its derivatives, achieving desirable drug release profiles.

# References


1. Graham, T., *XXXV.-On the properties of silicic acid and other analogous colloidal substances.* Journal of the Chemical Society, 1864. **17**(0): p. 318-327.
2. Graham, T., *Liquid Diffusion Applied to Analysis.* Philosophical Transactions of the Royal Society of London, 1861. **151**: p. 183-224.
3. Almdal, K., et al., *Towards a phenomenological definition of the term 'gel'.* Polymer Gels and Networks, 1993. **1**(1): p. 5-17.
4. Ferry, J.D., *Viscoelastic Properties of Polymers*. 3rd ed. 1980, New York, USA: John Wiley & Sons.
5. Burchard, W. and S.B. Ross-Murphy, *Introduction: physical gels from synthetic and biological macromolecules*, in *Physical Networks: Polymers and Gels*, W. Burchard and S.B. Ross-Murphy, Editors. 1990, Elsevier Applied Science: London, UK. p. 1-14.
6. Hennink, W.E. and C.F. van Nostrum, *Novel crosslinking methods to design hydrogels.* Advanced Drug Delivery Reviews, 2002. **54**(1): p. 13-36.
7. Peppas, N.A., et al., *Hydrogels in pharmaceutical formulations.* European Journal of Pharmaceutics and Biopharmaceutics, 2000. **50**(1): p. 27-46.
8. Hoare, T.R. and D.S. Kohane, *Hydrogels in drug delivery: Progress and challenges.* Polymer, 2008. **49**(8): p. 1993-2007.
9. Lin, C.-C. and A.T. Metters, *Hydrogels in controlled release formulations: Network design and mathematical modeling.* Advanced Drug Delivery Reviews, 2006. **58**(12–13): p. 1379-1408.
10. Hoffman, A.S., *Hydrogels for biomedical applications.* Advanced Drug Delivery Reviews, 2012. **64, Supplement**(0): p. 18-23.
11. Lee, K.Y. and S.H. Yuk, *Polymeric protein delivery systems.* Progress in Polymer Science, 2007. **32**(7): p. 669-697.
12. Bittner, B., et al., *Degradation and protein release properties of microspheres prepared from biodegradable poly(lactide-co-glycolide) and ABA triblock copolymers: influence of buffer media on polymer erosion and bovine serum albumin release.* Journal of Controlled Release, 1999. **60**(2–3): p. 297-309.
13. DuBose, J.W., C. Cutshall, and A.T. Metters, *Controlled release of tethered molecules via engineered hydrogel degradation: Model development and validation.* Journal of Biomedical Materials Research Part A, 2005. **74A**(1): p. 104-116.
14. Li, L., et al., *Reexamining the Egg-Box Model in Calcium–Alginate Gels with X-ray Diffraction.* Biomacromolecules, 2007. **8**(2): p. 464-468.
15. Amsden, B. and N. Turner, *Diffusion characteristics of calcium alginate gels.* Biotechnology and Bioengineering, 1999. **65**(5): p. 605-610.
16. Martinsen, A., G. Skjåk-Bræk, and O. Smidsrød, *Alginate as immobilization material: I. Correlation between chemical and physical properties of alginate gel beads.* Biotechnology and Bioengineering, 1989. **33**(1): p. 79-89.
17. Peppas, N.A. and J.E. Scott, *Controlled release from poly ( vinyl alcohol ) gels prepared by freezing-thawing processes.* Journal of Controlled Release, 1992. **18**(2): p. 95-100.
18. Takamura, A., F. Ishii, and H. Hidaka, *Drug release from poly(vinyl alcohol) gel prepared by freeze-thaw procedure.* Journal of Controlled Release, 1992. **20**(1): p. 21-27.
19. Ikada, Y., et al., *Stereocomplex formation between enantiomeric poly(lactides).* Macromolecules, 1987. **20**(4): p. 904-906.
20. Jeong, B., S.W. Kim, and Y.H. Bae, *Thermosensitive sol–gel reversible hydrogels.* Advanced Drug Delivery Reviews, 2002. **54**(1): p. 37-51.
21. Lee, K.Y., et al., *Controlling Mechanical and Swelling Properties of Alginate Hydrogels Independently by Cross-Linker Type and Cross-Linking Density.* Macromolecules, 2000. **33**(11): p. 4291-4294.

22. Watanabe, J., et al., *Preparation and characterization of poly(ethylene glycol) hydrogels cross-linked by hydrolyzable polyrotaxane.* Journal of Biomaterials Science, Polymer Edition, 2000. **11**(12): p. 1333-1345.
23. Bouhadir, K.H., et al., *Degradation of Partially Oxidized Alginate and Its Potential Application for Tissue Engineering.* Biotechnology Progress, 2001. **17**(5): p. 945-950.
24. Peppas, N.A. and R.E. Berner Jr, *Proposed method of intracopdal injection and gelation of poly (vinyl alcohol) solution in vocal cords: polymer considerations.* Biomaterials, 1980. **1**(3): p. 158-162.
25. Berger, J., et al., *Structure and interactions in covalently and ionically crosslinked chitosan hydrogels for biomedical applications.* European Journal of Pharmaceutics and Biopharmaceutics, 2004. **57**(1): p. 19-34.
26. WICHTERLE, O. and D. LIM, *Hydrophilic Gels for Biological Use.* Nature, 1960. **185**: p. 117-118.
27. Sperinde, J.J. and L.G. Griffith, *Synthesis and Characterization of Enzymatically-Cross-Linked Poly(ethylene glycol) Hydrogels.* Macromolecules, 1997. **30**(18): p. 5255-5264.
28. Westhaus, E. and P.B. Messersmith, *Triggered release of calcium from lipid vesicles: a bioinspired strategy for rapid gelation of polysaccharide and protein hydrogels.* Biomaterials, 2001. **22**(5): p. 453-462.
29. Kuijpers, A.J., et al., *Characterization of the Network Structure of Carbodiimide Cross-Linked Gelatin Gels.* Macromolecules, 1999. **32**(10): p. 3325-3333.
30. Peppas, N.A. and E.W. Merrill, *Crosslinked poly(vinyl alcohol) hydrogels as swollen elastic networks.* Journal of Applied Polymer Science, 1977. **21**(7): p. 1763-1770.
31. Brannon-Peppas, L. and N.A. Peppas, *Equilibrium swelling behavior of pH-sensitive hydrogels.* Chemical Engineering Science, 1991. **46**(3): p. 715-722.
32. Anseth, K.S., C.N. Bowman, and L. Brannon-Peppas, *Mechanical properties of hydrogels and their experimental determination.* Biomaterials, 1996. **17**(17): p. 1647-1657.
33. Eiselt, P., K.Y. Lee, and D.J. Mooney, *Rigidity of Two-Component Hydrogels Prepared from Alginate and Poly(ethylene glycol)–Diamines.* Macromolecules, 1999. **32**(17): p. 5561-5566.
34. Meyvis, T.K.L., et al., *Rheological monitoring of long-term degrading polymer hydrogels.* Journal of Rheology, 1999. **43**(4): p. 933-950.
35. Canal, T. and N.A. Peppas, *Correlation between mesh size and equilibrium degree of swelling of polymeric networks.* Journal of Biomedical Materials Research, 1989. **23**(10): p. 1183-1193.
36. Mason, M.N., et al., *Predicting Controlled-Release Behavior of Degradable PLA-b-PEG-b-PLA Hydrogels.* Macromolecules, 2001. **34**(13): p. 4630-4635.
37. SCHURZ, J., *Rheology of polymer solutions of the network type.* Progress in polymer science, 1991. **16**(1): p. 1-53.
38. Lee, W., et al., *Preparation of micropatterned hydrogel substrate via surface graft polymerization combined with photolithography for biosensor application.* Sensors and Actuators B: Chemical, 2008. **129**(2): p. 841-849.
39. Hoffmann, J., et al., *Photopatterning of thermally sensitive hydrogels useful for microactuators.* Sensors and Actuators A: Physical, 1999. **77**(2): p. 139-144.
40. Eddington, D.T. and D.J. Beebe, *Flow control with hydrogels.* Advanced Drug Delivery Reviews, 2004. **56**(2): p. 199-210.
41. Wen, Y. and S.-T. Yang, *The future of microfluidic assays in drug development.* Expert Opinion on Drug Discovery, 2008. **3**(10): p. 1237-1253.
42. Langer, R. and J. Vacanti, *Tissue engineering.* Science, 1993. **260**(5110): p. 920-926.
43. Kohane, D.S. and R. Langer, *Polymeric Biomaterials in Tissue Engineering.* Pediatr Res, 2008. **63**(5): p. 487-491.

44. Kuo, C.K. and P.X. Ma, *Ionically crosslinked alginate hydrogels as scaffolds for tissue engineering: Part 1. Structure, gelation rate and mechanical properties.* Biomaterials, 2001. **22**(6): p. 511-521.
45. Chung, H.J. and T.G. Park, *Surface engineered and drug releasing pre-fabricated scaffolds for tissue engineering.* Advanced Drug Delivery Reviews, 2007. **59**(4–5): p. 249-262.
46. Schmidt, J.J., J. Rowley, and H.J. Kong, *Hydrogels used for cell-based drug delivery.* Journal of Biomedical Materials Research Part A, 2008. **87A**(4): p. 1113-1122.
47. Cruise, G.M., D.S. Scharp, and J.A. Hubbell, *Characterization of permeability and network structure of interfacially photopolymerized poly(ethylene glycol) diacrylate hydrogels.* Biomaterials, 1998. **19**(14): p. 1287-1294.
48. Kong, H.J. and D.J. Mooney, *The Effects of Poly(Ethyleneimine) (PEI) Molecular Weight on Reinforcement of Alginate Hydrogels.* Cell Transplantation, 2003. **12**(7): p. 779-785.
49. Kloxin, A.M., et al., *Mechanical Properties of Cellularly Responsive Hydrogels and Their Experimental Determination.* Advanced Materials, 2010. **22**(31): p. 3484-3494.
50. Bhattarai, N., J. Gunn, and M. Zhang, *Chitosan-based hydrogels for controlled, localized drug delivery.* Advanced Drug Delivery Reviews, 2010. **62**(1): p. 83-99.
51. Qiu, Y. and K. Park, *Environment-sensitive hydrogels for drug delivery.* Advanced Drug Delivery Reviews, 2001. **53**(3): p. 321-339.
52. Amsden, B., *Solute Diffusion within Hydrogels. Mechanisms and Models.* Macromolecules, 1998. **31**(23): p. 8382-8395.
53. Masaro, L. and X.X. Zhu, *Physical models of diffusion for polymer solutions, gels and solids.* Progress in Polymer Science, 1999. **24**(5): p. 731-775.
54. Amsden, B., *Solute diffusion in hydrogels.: An examination of the retardation effect.* Polymer Gels and Networks, 1998. **6**(1): p. 13-43.
55. Crank, J., *The Mathematics of Diffusion*. Second ed. 1975, Oxford: Clarendon Press.
56. Miyata, T., N. Asami, and T. Uragami, *A reversibly antigen-responsive hydrogel.* Nature, 1999. **399**(6738): p. 766-769.
57. Tønnesen, H.H. and J. Karlsen, *Alginate in Drug Delivery Systems.* Drug Development and Industrial Pharmacy, 2002. **28**(6): p. 621-630.
58. Moebus, K., J. Siepmann, and R. Bodmeier, *Alginate–poloxamer microparticles for controlled drug delivery to mucosal tissue.* European Journal of Pharmaceutics and Biopharmaceutics, 2009. **72**(1): p. 42-53.
59. Funami, T., et al., *Rheological properties of sodium alginate in an aqueous system during gelation in relation to supermolecular structures and Ca2+ binding.* Food Hydrocolloids, 2009. **23**(7): p. 1746-1755.
60. Lee, K.Y. and D.J. Mooney, *Alginate: Properties and biomedical applications.* Progress in Polymer Science, 2012. **37**(1): p. 106-126.
61. Ibáñez, J.P. and Y. Umetsu, *Potential of protonated alginate beads for heavy metals uptake.* Hydrometallurgy, 2002. **64**(2): p. 89-99.
62. Krasaekoopt, W., B. Bhandari, and H. Deeth, *The influence of coating materials on some properties of alginate beads and survivability of microencapsulated probiotic bacteria.* International Dairy Journal, 2004. **14**(8): p. 737-743.
63. Grant, G.T., et al., *Biological interactions between polysaccharides and divalent cations: The egg-box model.* FEBS Letters, 1973. **32**(1): p. 195-198.
64. Atkins, E.D.T., et al., *Structural components of alginic acid. II. The crystalline structure of poly-α-L-guluronic acid. Results of X-ray diffraction and polarized infrared studies.* Biopolymers, 1973. **12**(8): p. 1879-1887.
65. Smeds, K.A. and M.W. Grinstaff, *Photocrosslinkable polysaccharides for in situ hydrogel formation.* Journal of Biomedical Materials Research, 2001. **54**(1): p. 115-121.

66. Lee, K.Y., et al., *Hydrogel Formation via Cell Crosslinking.* Advanced Materials, 2003. **15**(21): p. 1828-1832.
67. Zhao, S., et al., *Synthesis and characterization of thermo-sensitive semi-IPN hydrogels based on poly(ethylene glycol)-co-poly(ε-caprolactone) macromer, N-isopropylacrylamide, and sodium alginate.* Carbohydrate Research, 2010. **345**(3): p. 425-431.
68. Yu, C.-Y., et al., *Sustained release of antineoplastic drugs from chitosan-reinforced alginate microparticle drug delivery systems.* International Journal of Pharmaceutics, 2008. **357**(1–2): p. 15-21.
69. Zhang, X., et al., *Alginate microsphere filled with carbon nanotube as drug carrier.* International Journal of Biological Macromolecules, 2010. **47**(3): p. 389-395.
70. Wang, Q., et al., *Alginate/starch blend fibers and their properties for drug controlled release.* Carbohydrate Polymers, 2010. **82**(3): p. 842-847.
71. Augst, A.D., H.J. Kong, and D.J. Mooney, *Alginate Hydrogels as Biomaterials.* Macromolecular Bioscience, 2006. **6**(8): p. 623-633.
72. Gu, F., B. Amsden, and R. Neufeld, *Sustained delivery of vascular endothelial growth factor with alginate beads.* Journal of Controlled Release, 2004. **96**(3): p. 463-472.
73. EHTEDA, A., et al., *Complexation of Albendazole with Hydroxypropyl-β-Cyclodextrin Significantly Improves its Pharmacokinetic Profile, Cell Cytotoxicity and Antitumor Efficacy in Nude Mice.* Anticancer Research, 2012. **32**(9): p. 3659-3666.
74. Wang, F.-Q., et al., *A novel pH-sensitive magnetic alginate–chitosan beads for albendazole delivery.* Drug Development and Industrial Pharmacy, 2010. **36**(7): p. 867-877.
75. Hossein Pourgholami, M., et al., *Albendazole: a Potent Inhibitor of Vascular Endothelial Growth Factor and Malignant Ascites Formation in OVCAR-3 Tumor-Bearing Nude Mice.* Clinical Cancer Research, 2006. **12**(6): p. 1928-1935.
76. POURGHOLAMI, M.H., K.T. WANGOO, and D.L. MORRIS, *Albendazole-Cyclodextrin Complex: Enhanced Cytotoxicity in Ovarian Cancer Cells.* Anticancer Research, 2008. **28**(5A): p. 2775-2779.
77. Pourgholami, M., et al., *Antitumor activity of albendazole against the human colorectal cancer cell line HT-29: in vitro and in a xenograft model of peritoneal carcinomatosis.* Cancer Chemotherapy and Pharmacology, 2005. **55**(5): p. 425-432.
78. Behrend, R., E. Meyer, and F. Rusche, *I. Ueber Condensationsproducte aus Glycoluril und Formaldehyd.* Justus Liebigs Annalen der Chemie, 1905. **339**(1): p. 1-37.
79. Freeman, W.A., W.L. Mock, and N.Y. Shih, *Cucurbituril.* Journal of the American Chemical Society, 1981. **103**(24): p. 7367-7368.
80. Zhao, Y., *Cucurbit[n]uril - a delivery host for anti-cancer drugs*, in *School of Physical, Environmental and Mathematical Sciences*2009, Australian Defence Force Academy, University of New South Wales.
81. Day, A., A. Arnold, and R. Blanch, *A Method for Synthesizing Partially Substituted Cucurbit[n]uril.* Molecules, 2003. **8**(1): p. 74-84.
82. Zhao, Y., et al., *Synthesis of a symmetrical tetrasubstituted cucurbit[6]uril and its host-guest inclusion complex with 2,2′-bipyridine.* Chinese Science Bulletin, 2004. **49**(11): p. 1111-1116.
83. Isaacs, L., *Approaches to drug delivery based on the principles of supramolecular chemistry.* Advanced Drug Delivery Reviews, 2012. **64**(9): p. 763.
84. Ghosh, I. and W.M. Nau, *The strategic use of supramolecular pKa shifts to enhance the bioavailability of drugs.* Advanced Drug Delivery Reviews, 2012. **64**(9): p. 764-783.
85. Day, A.I. and J.G. Collins, *Cucurbituril Receptors and Drug Delivery*, in *Supramolecular Chemistry*. 2012, John Wiley & Sons, Ltd.

86. Lagona, J., et al., *The Cucurbit[n]uril Family.* Angewandte Chemie International Edition, 2005. **44**(31): p. 4844-4870.
87. Day, A., et al., *Controlling Factors in the Synthesis of Cucurbituril and Its Homologues.* The Journal of Organic Chemistry, 2001. **66**(24): p. 8094-8100.
88. Walker, S., et al., *The Potential of Cucurbit[n]urils in Drug Delivery.* Israel Journal of Chemistry, 2011. **51**(5-6): p. 616-624.
89. Hoffmann, R., et al., *Host-guest complexes of cucurbituril with the 4-methylbenzylammonium lon, alkali-metal cations and NH4+.* Journal of the Chemical Society, Faraday Transactions, 1994. **90**(11): p. 1507-1511.
90. Buschmann, H.J., E. Cleve, and E. Schollmeyer, *Cucurbituril as a ligand for the complexation of cations in aqueous solutions.* Inorganica Chimica Acta, 1992. **193**(1): p. 93-97.
91. Buschmann, H.-J., et al., *The formation of alkali and alkaline earth cation complexes with cucurbit[6]uril in aqueous solution: a critical survey of old and new results.* Journal of Inclusion Phenomena and Macrocyclic Chemistry, 2009. **65**(3-4): p. 293-297.
92. Kanjickal, D., et al., *Improving delivery of hydrophobic drugs from hydrogels through cyclodextrins.* Journal of Biomedical Materials Research Part A, 2005. **74A**(3): p. 454-460.
93. Jeon, W.S., et al., *Complexation of Ferrocene Derivatives by the Cucurbit[7]uril Host: A Comparative Study of the Cucurbituril and Cyclodextrin Host Families.* Journal of the American Chemical Society, 2005. **127**(37): p. 12984-12989.
94. Fahr, A. and X. Liu, *Drug delivery strategies for poorly water-soluble drugs.* Expert Opinion on Drug Delivery, 2007. **4**(4): p. 403-416.
95. Uzunova, V.D., et al., *Toxicity of cucurbit[7]uril and cucurbit[8]uril: an exploratory in vitro and in vivo study.* Organic and Biomolecular Chemistry, 2010. **8**: p. 2037-2042.
96. Ge, J.-Y., et al., *Interaction of Cucurbit[n = 6∼8]urils and Benzimidazole Derivatives.* Journal of Inclusion Phenomena and Macrocyclic Chemistry, 2007. **58**(1-2): p. 63-69.
97. Day, A., et al., *The Effects of Alkali Metal Cations on Product Distributions in Cucurbit[n]uril Synthesis.* Journal of Inclusion Phenomena and Macrocyclic Chemistry, 2002. **43**(3-4): p. 247-250.
98. Oswal, A., et al., *Validated UV Spectrophotometric Method for Estimation of Albendazole in Tablet Dosage Form.* Journal of Pharmacy Research, 2010. **3**(6): p. 1355-1357.
99. Xu, Y., et al., *Preparation of dual crosslinked alginate–chitosan blend gel beads and in vitro controlled release in oral site-specific drug delivery system.* International Journal of Pharmaceutics, 2007. **336**(2): p. 329-337.
100. Shi, J., N.M. Alves, and J.F. Mano, *Drug Release of pH/Temperature-Responsive Calcium Alginate/Poly(N-isopropylacrylamide) Semi-IPN Beads.* Macromolecular Bioscience, 2006. **6**(5): p. 358-363.
101. Kim, M.S., et al., *Ionically crosslinked alginate–carboxymethyl cellulose beads for the delivery of protein therapeutics.* Applied Surface Science, 2012. **262**(0): p. 28-33.
102. Istini, S., M. Ohno, and H. Kusunose, *Methods of analysis for agar, carrageenan and alginate in seaweed.* Bulletin of marine sciences and fisheries, Kochi University, 1994(14): p. 49-55.
103. Okuzaki, H. and Y. Osada, *Effects of hydrophobic interaction on the cooperative binding of a surfactant to a polymer network.* Macromolecules, 1994. **27**(2): p. 502-506.
104. Okuzaki, H. and Y. Osada, *Role and Effect of Cross-Linkage on the Polyelectrolyte-Surfactant Interactions.* Macromolecules, 1995. **28**(13): p. 4554-4557.
105. Okuzaki, H., Y. Eguchi, and Y. Osada, *Size Effect of the Alkyl Chain of the Surfactant on the Chemomechanical Movement of a Polymer Gel.* Chemistry of Materials, 1994. **6**(10): p. 1651-1653.

106. Caram-Lelham, N. and L.-O. Sundelöf, *Changes in the polyelectrolyte-amphiphile interaction due to helix-coil transition induced by specific counterions or variations in temperature.* Biopolymers, 1996. **39**(3): p. 387-393.
107. Hayakawa, K. and J.C.T. Kwak, *Surfactant-polyelectrolyte interactions. 1. Binding of dodecyltrimethylammonium ions by sodium dextransulfate and sodium poly(styrenesulfonate) in aqueous solution in the presence of sodium chloride.* The Journal of Physical Chemistry, 1982. **86**(19): p. 3866-3870.
108. Malovikova, A., K. Hayakawa, and J.C.T. Kwak, *Surfactant-polyelectrolyte interactions. 4. Surfactant chain length dependence of the binding of alkylpyridinium cations to dextran sulfate.* The Journal of Physical Chemistry, 1984. **88**(10): p. 1930-1933.
109. Day, A.I., et al., *A Cucurbituril-Based Gyroscane: A New Supramolecular Form.* Angewandte Chemie International Edition, 2002. **41**(2): p. 275-277.
110. Feng, X., et al., *Stable cucurbit[5]uril MOF structures as 'beaded' rings built on a p-hydroxybenzoic acid template-a small molecule absorption material.* CrystEngComm, 2011. **13**(16): p. 5049-5051.
111. Siepmann, J. and N.A. Peppas, *Higuchi equation: Derivation, applications, use and misuse.* International Journal of Pharmaceutics, 2011. **418**(1): p. 6-12.
112. Siepmann, J. and F. Siepmann, *Modeling of diffusion controlled drug delivery.* Journal of Controlled Release, 2012. **161**(2): p. 351-362.
113. Korsmeyer, R.W., et al., *Mechanisms of solute release from porous hydrophilic polymers.* International Journal of Pharmaceutics, 1983. **15**(1): p. 25-35.
114. Mellott, M.B., K. Searcy, and M.V. Pishko, *Release of protein from highly cross-linked hydrogels of poly(ethylene glycol) diacrylate fabricated by UV polymerization.* Biomaterials, 2001. **22**(9): p. 929-941.
115. Rasmussen, M.R., T. Snabe, and L.H. Pedersen, *Numerical modelling of insulin and amyloglucosidase release from swelling Ca–alginate beads.* Journal of Controlled Release, 2003. **91**(3): p. 395-405.
116. Wu, F., et al., *Locating the Cyclopentano Cousins of the Cucurbit[n]uril Family.* The Journal of Organic Chemistry, 2011. **77**(1): p. 606-611.
117. Rekharsky, M.V., et al., *A synthetic host-guest system achieves avidin-biotin affinity by overcoming enthalpy–entropy compensation.* Proceedings of the National Academy of Sciences, 2007. **104**(52): p. 20737-20742.